

AD-A170 484

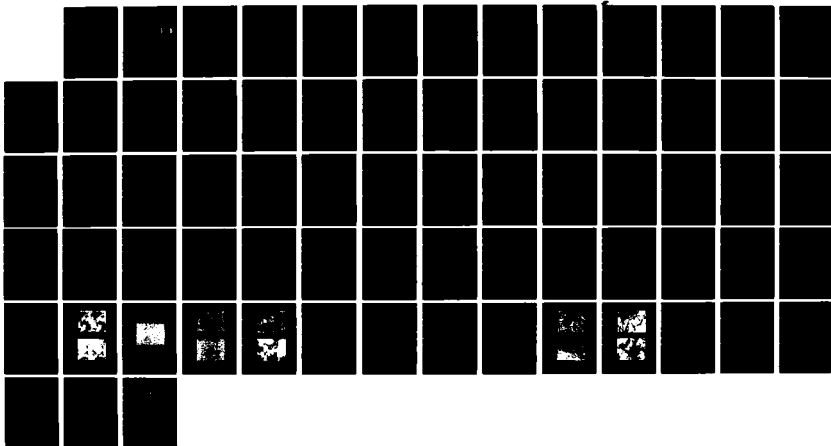
AN INTERDISCIPLINARY APPROACH TO PREDICTIVE MODELING OF
STRUCTURAL ADHESI (U) VIRGINIA TECH CENTER FOR
ADHESION SCIENCE BLACKSBURG J A FILBEY ET AL MAY 86
CAS/CHEM-4-86 N00014-82-K-0185

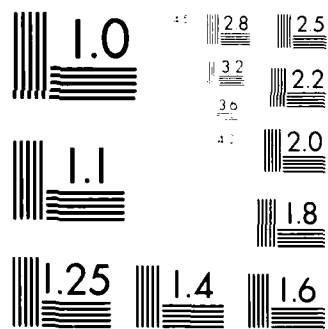
1/1

UNCLASSIFIED

F/G 11/1

NL





MICROCOPY RESOLUTION TEST CHART

NATIONAL BUREAU OF STANDARDS-1963-A

AD-A170 484

12

No. 86
CAS/CHEM-4-86

**VIRGINIA TECH
CENTER FOR ADHESION SCIENCE**

DTIC
ELECTE
JUL 3 1 1986
S **D**
D

ANNUAL REPORT

AN INTERDISCIPLINARY APPROACH TO PREDICTIVE
MODELING OF STRUCTURAL ADHESIVE BONDING

CHARACTERIZATION OF Ti-6Al-4V OXIDES AND
THE ADHESIVE/OXIDE INTERPHASE

BY

J. A. FILBEY AND J. P. WIGHTMAN

DISTRIBUTION STATEMENT A

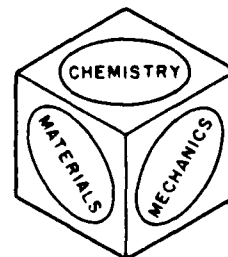
Approved for public release
Distribution Unlimited

DTIC FILE COPY

VIRGINIA POLYTECHNIC INSTITUTE
AND STATE UNIVERSITY

216 NORRIS HALL
BLACKSBURG, VIRGINIA 24061

Telephone: (703) 961-6824
TLX: 9103331861



ANNUAL REPORT

AN INTERDISCIPLINARY APPROACH TO PREDICTIVE MODELING
OF STRUCTURAL ADHESIVE BONDING

CHARACTERIZATION OF Ti-6Al-4V OXIDES AND THE
ADHESIVE/OXIDE INTERPHASE

BY

J. A. FILBEY AND J. P. WIGHTMAN

PREPARED FOR

OFFICE OF NAVAL RESEARCH
800 NORTH QUINCY STREET
ARLINGTON, VIRGINIA 22178

DR. L. H. PEEBLES, JR.

GRANT NO. N00014-82-K-0185 PC0002

FROM

CENTER FOR ADHESION SCIENCE
VIRGINIA POLYTECHNIC INSTITUTE AND STATE UNIVERSITY
BLACKSBURG, VIRGINIA 24061

MAY, 1986*

*This report covers research done during the period 6-18-84 to 9-18-85.

I. INTRODUCTION

Ti-6-4, being a high strength, lightweight, corrosion resistant alloy, possesses many uses for structural adhesive bonding. Many researchers are therefore finding better pretreatments, characterizing the oxide surface and evaluating bonding performance [1-5]. The work reported here will encompass both oxide characterization and evaluation of adhesive bonds. The chemical composition of oxides created by specific pretreatments was studied by XPS*, AES, SIMS, contact angles, and indicator dyes. The surface topography and structure was probed by SEM, STEM, and profilometry. Following the procedures of Carre and Schultz with aluminum substrates [6], values for the surface energy of the Ti-6-4 oxides are obtained using an interfacial contact angle method. Because of the present interest in the use of Ti-6-4 for high temperature applications, the thermal stability of the oxide layer was investigated. Following Pike's successful use of inorganic primers as adhesion promoters on aluminum substrates [7], studies were begun to characterize a titanate primer. Finally, both lap shear and wedge tests have been used to evaluate the adhesive/oxide interphase.

II. EXPERIMENTAL

A. Surface Pretreatments

Oxide layers were created on the Ti-6-4 surfaces of the lap shear coupons, wedge samples and foil by one of the following pretreatments: a 10 volt chromic acid anodization (CAA), a 10 volt sodium hydroxide anodization (SHA)[1], a phosphate-fluoride acidic etch (P/F), or the TURCO 5578 basic etch. If a pickling step used in the CAA treatment preceded the TURCO or SHA

*Acronyms are defined in the next section.



<input checked="" type="checkbox"/> <input type="checkbox"/> <input type="checkbox"/>	
<i>etc. on file</i>	
Availability Codes	
Dist	Avail and/or Special
A-1	

pretreatments, the designations PTURCO or PSHA will be used. The procedures for each of these pretreatments and the modifications made when the Ti-6-4 foil was used are listed in Appendix A.

B. Auger Electron Spectroscopy, AES

AES was done exclusively on a Perkin-Elmer PHI 610 scanning Auger microprobe with an electron beam voltage of 3 to 5 kV and a beam current of 0.05 μ a. Narrow scan surveys were taken from 300 ev to 600 ev. Samples were depth profiled by Argon ion sputtering with an ion beam voltage of 4 kV, an emission current of 25 ma and an ion beam current of 0.2 μ a.

C. Secondary Ion Mass Spectroscopy, SIMS

Dynamic SIMS spectra were obtained on a Perkin-Elmer PHI 3500 mass spectrometry. Mass to charge ratios ranged from 1 to 200 amu. Spectra were taken with and without an inbleed of oxygen gas.

D. X-ray Photoelectron Spectroscopy, XPS

XPS analysis was obtained on both a KRATOS XSAM 800 spectrometer and a PHI 5300 ESCA system using a Mg anode. Samples were punched as 0.95 cm (0.38 in.) disks and scanned from 0 to 1200 ev. Narrow scans were routinely made on any significant peaks seen in the wide scan spectra.

E. Roughness

Comparative roughness of the three pretreated Ti-6-4 foil samples was determined by profilometry. A Taylor-Hobson Talysurf 4 profilometer gave the average height at half width of the peak to valley profile as measured with a diamond stylus. These measurements were compared to those previously done on the Ti-6-4 pretreated coupon surfaces.

F. Surface Free Energy Determination

The Ti-6-4 surfaces were pretreated by one of the four pretreatments: CAA, P/F, TURCO, or PTURCO. After drying with dry nitrogen gas, the surfaces were placed in a hot plate oven at 110°C for at least 48 hours. The oven was then turned off and the surfaces allowed to cool to room temperature. The contact angle of a water drop placed on a pretreated Ti-6-4 sample immersed in an alkane was measured. A series of four alkanes was used: hexane, octane, decane, and hexadecane. From the contact angle measurements, the dispersive and polar components of the surface free energy were obtained by the calculations outlined in Figure 1 [6].

G. Scanning Transmission Electron Microscopy, STEM

STEM pictures were obtained on a Phillips EM-420T electron microscope. Ti-6-4 foil was pretreated and cut to 3 by 8 mm (0.12 - 0.31 inch) pieces. The magnifications ranged from 3200 to 100,000 times. Gold coating of the samples was not necessary.

H. Scanning Electron Microscopy, SEM

SEM photomicrographs were taken on a JEOL JSM-35-c electron microscope. Pretreated samples were punched as 0.95 cm (0.38 inch) disks and sputter coated with gold, resulting in a coating of 20 nm.

Stereophotomicrographs were also taken. At 200 x and at the tilt of interest, the sample was focused. A spot on the sample was aligned with a center point marked on the screen. The z axis was also adjusted so that the spot chosen on the sample remained in line with the center point on the screen when the tilt axis was rotated +/- a few degrees. The sample was photographed at the magnification desired. The sample was then tilted +/- 7 degrees while

keeping the spot on the sample aligned with the center spot of the screen using the x and y axis controls. A second picture was taken. The pictures can then be aligned next to one another, placing the higher angle photograph on the left side.

I. Acidity/Basicity

A series of indicator dyes was used on all the pretreated surfaces [5]. Bromthymol blue solution (LaMotte Chemical Products) was used as received. 0.01 g of Orange 1, Thymol blue (both Pfaltz and Bauer, Inc), and Bromphenol blue (Arthur H. Thomas Co) were dissolved in 25 ml. of deionized water. 0.1 g of Bromcresol purple (Chemical Dynamics Corporation) was dissolved in 9.25 ml of 0.02 N NaOH and diluted to 250 ml. The color of each dye after contact with the dry pretreated surface was observed.

J. Bonding

Lap shear joints were bonded with four layers of FM-300U epoxy. The bonding cycle included heating from room temperature to 175°C (350°F) using 13.8 MPa (2,000 psi) bonding pressure. The 175°C temperature was held for 1.5 hours before cooling to room temperature and removing from the press.

Wedge samples were bonded with two layers of epoxy with three layers of teflon film used as spacers, yielding a bond thickness of .0381 cm (0.015 in.). The bonding cycle included heating from room temperature to 175°C (350°F) using 1.72 MPa (250 psi) bonding pressure. The 175°C temperature was held for 1.5 hours before cooling to room temperature and removing from the press. After bonding, a wedge made of Ti-6-4 was driven into one end of the sample, causing an initial crack to propagate. Samples were then placed into one of three environments held at 80°C: 95% r.h., water immersion, or 0.5 M

basic phosphate buffer immersion, pH = 11.0. The basic buffer consisted of 268.07 g of $\text{Na}_2\text{HPO}_4 \cdot 7\text{H}_2\text{O}$ and 380.12 g of $\text{Na}_3\text{HPO}_4 \cdot 12\text{H}_2\text{O}$ (Fisher Scientific) per 2 liters of water. Periodically, the position of the crack was measured manually with a ruler.

K. Sample Preparation for IR

Polished Ti-6-4 samples were prepared from lap shear coupons. 2.54 cm (1 inch) disks were cut and placed in brass holders. 2.54 cm (1 inch) disks were cut and placed in brass holders. A series of polishing wheels were used, stepping to the next finer grit only when the disk was covered with uniform scratches. The final wheel grit size was 0.05 μm . In the last step, the polished disks were placed in a vibrating bath contained Buehler Mastermet colloidal silica, allowing the samples to vibrate overnight.

A Ken React LICA 38 titanate primer was used as a 0.2 wt % solution in isopropanol. The polished pieces were dried in air after dipping in the primer solution.

L. Infrared Spectroscopy

A Nicolet 5DX FTIR spectrometer was used with a grazing angle specular reflectance attachment. A single diamond polarizer was used to create plane polarized light parallel to the plane of incidence. The chamber was purged with nitrogen gas for 30 min. before spectra were obtained.

III. RESULTS AND DISCUSSION

A. Oxide Chemical Composition of Pretreated Surfaces

The chemical composition of the oxide surfaces created by CAA, SHA, PSHA,

P/F, and TURCO on Ti-6-4 coupons was studied by XPS, AES, SIMS and indicator dyes.

XPS yields information on the elemental identity as well as the bonding state of the species present on approximately the top 5 nm of the surface. Chemical reproducibility of the surface pretreatments can be investigated by XPS. The elements on the pretreated surface, the binding energies (in eV) and atomic fractions are listed for each pretreatment in Table I. As this reproducibility study is a continuation from the previous report [4], a statistical treatment of the atomic fractions, X/Ti ratios and binding energies on the data from both reports is presented in Table II. The confidence limits for the average atomic fractions encompass a relatively large range over which the mean can fall. This large range is due in part to sample to sample variation of the inherent contamination layer. Even so, the variation is typically <10% even at the 95% confidence level. The binding energies have confidence limits with narrow ranges, thus indicating good reproducibility of the chemical bonding state of the elements on the surface. A pictorial representation of the average atomic fractions resulting from each pretreatment is shown in Figure 2.

In addition to XPS, AES yields compositional information of the surface region. Wide scan spectra were collected for CAA, SHA, PSHA, P/F and TURCO pretreated surfaces. The elements detected and their kinetic energies are listed in Table III. The elements detected on the pretreated surfaces using AES agree with those detected using XPS. The characteristic elements for each pretreatment are: C, O, Ti and F for CAA; C, O, Ti and P for P/F; C, O, Ti, Fe and Si for TURCO; C, O, Ti, Ca, Si and P for SHA; and C, O, Ti, Ca and P for P.SHA.

Auger electron spectroscopy can also be used to determine the

stoichiometry of the Ti-6-4 oxides resulting from the pretreatments by comparison of narrow scans to spectra in the literature. The narrow scans for the CAA, P/F, TURCO, and SHA pretreated surfaces are shown in Figures 3 - 6. The peak shape between 400 and 420 eV of the four oxides appear very similar to one another. These spectra are compared to those of Roman et al. [8] and Solomon and Baun [9]. According to Roman, the difference between TiO and TiO₂ is determined in the 400 to 420 eV region. The spectra of all four of the oxides do not appear to match the peak shape TiO₂, but rather are similar to the TiO peak shape. However, M. Charbonnier and coworkers [10] have reported evidence for TiO₂ on anodized titanium surfaces using LEEIXS (Low energy electron induced x-ray spectroscopy).

Questions have arisen in the literature concerning the possibility of reduction of the oxide by the electron beam. Therefore, a narrow scan was taken of rutile TiO₂ powder, obtained from Dr. Parfitt from Carnegie-Mellon. The spectra is shown in Figure 7. The TiO₂ powder spectrum agrees with the TiO₂ spectrum of Solomon and Baun [9]. Thus, the powder did not reduce under the electron beam and the agreement although not incontrovertible, offers support of the stability of the Ti 6-4 oxides under the electron beam.

Another technique is available which yields information as to elements and groups of elements on the surface - Secondary Ion Mass Spectroscopy. Dynamic SIMS was performed on the CAA, P/F, TURCO, SHA, and PSHA surfaces. Tables IV to VIII list the peak position (at m/e values) and assignment of the positive ion spectrum. There are still unidentified peaks, some perhaps due to C_xH_y combinations from carbon contamination. Because of the wide range of sensitivity factors in the SIMS experiment, the peak intensities are not directly proportional to the amount present on the surface. Sodium is present in all spectra as a contaminant similar to the ubiquitous carbon in XPS. The

presence of aluminum is also detected, due to the higher sensitivity of the SIMS technique and the fact that profiling is occurring during the analysis. Fluorine is present on the CAA surface. Phosphorous is not detected on the P/F surface, perhaps because it forms a negatively charged ion or complex. The TURCO surface shows the presence of iron and silicon. Calcium and silicon are present on the sandblasted SHA surface in significant concentrations. Silicon is not as significant on the pickled SHA surfaces. These results are in agreement with results from XPS and AES experiments.

For comparison, a dynamic SIMS spectrum was obtained for rutile TiO_2 powder (from Dr. Parfitt). A tabulation of the peaks observed is found in Table IX. This allows for a cross check for peak identification and contamination due to the system. A peak at 56 amu, previously identified as iron is present and is thus perhaps inherent in the system.

Using XPS, AES, and SIMS, the elements present on the surface of the oxides have been established. The presence of hydrogen (or surface hydroxyls) remains elusive*. By determining the relative acidity/basicity of the pretreated surfaces another type of oxide composition information can be obtained. Indicator dyes are used to measure the acid/base nature of the oxide with the results listed in Table X. The two extremes are easily interpreted. The CAA surface is clearly acidic with the pH less than 3.4. The SHA surface is clearly basic with the pH above 8.0. P/F, TURCO, and PTURCO surfaces all exhibit a pH range between 5.2 and 7.6.

B. Oxide Topography and Structure

A variety of techniques can be used to investigate the topography and

*It is possible, using static SIMS to determine relative concentrations of Ti-OH with knowledge of the titanium isotope abundance when being sputtered.

structure of the surface oxide, namely SEM, STEM, AES with depth profiling and profilometry. The surface topography can be probed using electron microscopy. In the previous report [4], SEM photomicrographs of CAA, P/F and TURCO pretreated surfaces showed that the pretreatments yielded surfaces of different topographies. The SHA and PSHA pretreatments were investigated using SEM. Stereophotomicrographs are shown in Figure 8 and 9. These pretreatments also yielded different topographies. The PSHA surface appears to be a patchy version of the SHA surface. SEM, however, could not distinguish the presence of porosity. STEM was used to look at all of the pretreated surfaces with higher magnification and resolution. Figures 10 through 14 show STEM photomicrographs of all the pretreated surfaces. Porosity is seen in the CAA, SHA and PSHA pretreated surfaces. The porosity in the PSHA surface is better defined than the SHA surface. This is due to the fact that the current density is not controlled in the SHA and PSHA procedure. Because the barrier oxide has been diminished by the pickling step for the PSHA pretreatment, less resistance is present in the initial stage of the anodization step, thus forming better defined pores. The PSHA pores are quite similar in diameter to the CAA pores. No porosity is present in the P/F and TURCO surfaces.

STEM allows the topography and structure of the oxide to be seen at the nanometer level. This "roughness", however, is not quantified. Profilometry yields a quantitative measure of the surface roughness on a micron scale. The roughness results for the Ti-6-4 foil are listed in Table XI and compared with the roughness measurements previously taken on the Ti-6-4 coupons [4]. The foil is an order of magnitude smoother than the coupons with the P/F surface being slightly more rough than the CAA or TURCO.

Neither STEM nor profilometry give a measure of the thickness of the

oxide layer. The relative oxide thickness of the pretreated surfaces can be investigated using AES depth profiling. The average time taken for the oxygen and titanium signal to intersect for each pretreatment is listed in Table XII. A significantly longer time is required to sputter through the SHA oxides. It is thought that the long sputter time is not strictly due to thickness, but rather to a different sputter efficiency of the SHA oxide layer.

C. Surface Energy of Oxides

Both chemical composition and structure of the oxide layer play a role in surface energy determination. Using the interfacial contact angle method, hundreds of contact angle measurements were taken. The measurements were then treated statistically. After averaging the measurements for each alkane on each surface, those measurements falling outside a 95% confidence limit from the mean were discarded and a new average calculated. These average contact angles were used to graphically determine the dispersive and polar components of the surface free energy. The results are listed in Table XIII. The graphs for each pretreatment with error bars are shown in Figures 15 to 18. The PTURCO surface yields linear results, whereas the P/F, CAA and TURCO surfaces show deviation from linearity. Therefore a further calculation was done to determine, energetically, if the water drop was displacing the alkane which is in fact a requirement for the above treatment to be valid [11]. For displacement to be energetically predicted, the following relation must hold:

$$I_{sw}^P > 2[(\gamma_S^D)^{1/2} - (\gamma_H)^{1/2}][(\gamma_H)^{1/2} - (\gamma_W^D)^{1/2}] \quad [1]$$

All of the surfaces are predicted to have the water drop totally displace the alkane as shown in Table XIV. However, from profilometry measurements, the TURCO surface is found to be more rough than the other surfaces. From STEM,

the CAA surface is found to be porous. Therefore, due to considerations other than energetics, the water drop may not be totally displacing the alkane on the CAA and TURCO surfaces, thus perhaps accounting for the nonlinearity. This technique may not be valid for "rough", unpolished surfaces.

D. Effects of Heating on Ti-6-4 Oxides

XPS and STEM were used to study the effects of high temperature for a short duration of the oxides created by the pretreatments. Ti-6-4 foil was pretreated as described in Appendix I. The foil sample was then placed in the KRATOS spectrometer, heated to 350°C, held at that temperature for 10 minutes then cooled to room temperature, and spectra collected. Upon removal from the spectrometer, the sample was placed in the STEM for observation.

A listing of the elements detected, their binding energies and atomic fractions for the pretreated foils before and after heating is found in Tables XV through XVIII. An interesting phenomenon is observed in the titanium 2p photopeak shapes before and after heating. While no difference is seen in the CAA and SHA titanium peak shape after heating, the Ti peak for the P/F and TURCO oxide shows a broadening to the lower binding energy side. This broadening indicates a reduction in the oxide layer after heating for only ten minutes. A comparison of the two titanium signal is made in Figure 19.

Although chemical changes are seen in the P/F and TURCO spectra upon heating, STEM shows no visible physical change in topography for any of the pretreated oxides. STEM photomicrographs of the surfaces after heating are shown in Figures 20 through 23.

E. Inorganic Primers

The use of inorganic primers has been shown to enhance bond durability in

taluminum bonding [7]. Work has therefore begun in this lab to investigate titanate primers. Results from preliminary characterization studies will be reported here. The structure of LICA 38 (Ken Rich), a pyrophosphatotitanate, is shown in Figure 24. The infrared spectra of neat LICA 38 and as a film spun coat from a 1% isopropanol solution on polished Ti-6-4, taken with a grazing angle attachment are shown in Figures 25 and 26. The significant peaks are identified in Table IXX.

XPS was also used to study the inorganic primer film on polished Ti-6-4. A list of elements detected, binding energies, atomic fractions and curve fit data for the polished Ti-6-4 surface and for the LICA 38 film on the Ti-6-4 are found in Tables XX and XXI. The polished Ti-6-4 surface contains silicon oxide, a residual from the polishing. The titanium 2p peak only shows the presence of the oxide form of titanium. Once the primer is applied, the presence of silicon disappears implying the LICA 38 film is thicker than the analysis depth (5 nm). The presence of the titanium and the phosphorous are both from the primer. The oxygen peak is quite broad, in part due to the phosphate oxygens.

F. Structural Epoxy/Oxide Interphase

Two joint geometries were used to investigate the epoxy/oxide interaction. Lap shear bonds were made from coupons pretreated with CAA, P/F and TURCO are indistinguishable by lap shear strength as shown in Table XXI, thus re-emphasizing the inability of the lap shear test to evaluate surface pretreatments.

The wedge test, however, is sensitive to the surface pretreatment. Wedge samples were pretreated by CAA, SHA, TURCO, P/F, and P.TURCO and placed in a hydrothermal environment of 80°C and 100% r.h. CAA, SHA, and TURCO pretreated samples were tested for 14 days, 26 days, and 14 days, respectively and showed

no crack propagation over the test period. However, P/F and P.TURCO pretreated samples did show crack propagation. This crack propagation with time is shown in Figure 27. The strain energy release rate, G_I , can be calculated [3] using the equation:

$$G_I = \frac{y^2 Mh^3(3(a + 0.6h)^2 + h^2)}{16 ((a + 0.6h)^3 + ah^2)^2} \quad [2]$$

where: G_I = strain energy release rate (J/m²)
 y = displacement at load point (0.00381 m)
 a = distance from load point to crack tip
 h = height of beam (0.00381 m)
 M = modulus of beam (1.14E11 Pa)

Figure 28 shows a graph of da/dt vs. G_I for the P/F and P.TURCO data.

Two other environments were used with the wedge samples involving actual immersion of the samples. CAA, TURCO, and P/F pretreated samples were immersed in 80°C water for 49 days, 31 days and 2.5 hours, resp. Both the CAA and TURCO showed no crack propagation for the entire test period. The P/F pretreated samples failed in the same environment within 2.5 hours. TURCO pretreated samples were also immersed in a basic buffer for 17 days*. After 14 days, no crack propagation was seen; however, after 17 days a small crack of 0.3 cm was observed.

*Dr. Christopher Matz of MMB Transport Aircraft in Bremen, FRG suggested the user of acidic and basic buffers.neutral. The stoichiometry of the

IV. SUMMARY

The chemical composition of the surfaces created by the various pretreatments has been determined with excellent chemical reproducibility. The CAA surface is acidic, the SHA surface basic, the TURCO and P/F surfaces oxides do not appear to be TiO_2 with TiO indicated by AES. Porosity is present for both of the anodized surfaces, but depth profiling by AES indicates the sputter efficiency of the two similar looking oxide is quite different. Surface energy determination indicates Carre and Schultz's method is not readily amenable to Ti-6-4.

Lap shear reproducibility studies serve to reemphasize the inability of the lap shear geometry to distinguish between surface pretreatments. The use of accelerated wedge testing, by actual immersion of the wedge samples in buffer solutions has shown for the TURCO pretreated surfaces a reduction in the durability from 31 days (total time tested) to crack propagation in 17 days.

V. FUTURE WORK

The accelerated wedge test will be continuing with all pretreatments in both acidic and basic buffers at 80° and 95°C. Inorganic primers will also be used prior to adhesive bonding. Grazing angle infrared spectroscopy will be used to study thin films on reflective metal substrates such as polished Ti-6-4 and ferrotype plates.

VI. REFERENCES

1. A. C. Kennedy, R. Kohler and P. Poole. *Int. J. Adhesion and Adhesives*, 3, 133, 1983.
2. M. Natan and J. D. Venables. *J. Adhesion*, 15, 125, 1983.
3. S. R. Brown and G. J. Pilla, NADC-82032-60, March 31, 1982.
4. J. A. Filbey and J. P. Wightman. Annual Report, ONR, October, 1984.
5. J. G. Mason, R. Siriwardane and J. P. Wightman. *J. Adhesion*, 11, 315, 1981.
6. A. Carre and J. Sshultz. *J. Adhesion*, 15, 151, 1983.
7. R. A. Pike. *Int. J. Adhesion and Adhesives*, 5, 3, 1985.
8. E. Roman, M. Sanchez-Rvedillo and J. L. de Segovia. *Appl. Phys. A.*, 35, 35, 1984.
9. J. S. Solomon and W. L. Baun. *Surface Science*, 51, 228, 1975.
10. M. Charbonnier, M. Romand, A. Roche, F. Gaillard. ADHÉCOM, 1ère semaine internationale de l'adhésion et de l'assemblage. Bordeaux, France, April 15-18, 1986, p. 75.
11. parM. E. K. Shanahan, et.al. *J. de chimie Physique*, 79, n 3, 1982.

ACKNOWLEDGEMENTS

The authors would like to acknowledge the following people: Steve McCartney for running the KRATOS XPS and the STEM, Frank Cromer for help in data collection and training to run the PHI XPS and AES instruments. Dave Gilliam for training to use the profilometer. Lawrence Arney for help in the statistical treatment of the data.

The authors would like to acknowledge the Office of Naval Research and NASA-Langley Research Center for financial support of the work. The gift of titanium samples from RMI-Titanium was greatly appreciated.

APPENDIX I

Chromic Acid Anodization (CAA)

1. Gritblast with an Econoline gritblaster at approximately 100 psi and held approximately 5 cm from the coupon.
2. Wipe with methyl ethyl ketone (MEK).
3. Soak in sodium hydroxide solution (13g/250ml) at 70 C for 5 minutes.
4. Rinse three times in deionized water.
5. Pickling step: Immerse in pickle solution (15ml conc. HNO_3 , 3ml 49%w/w HF, 82ml H_2O) at room temperature for 5 minutes.
6. Rinse three times in deionized water.
7. Anodize at room temperature for 20 minutes at 10 volts, 26.9amp/sq.m (2.5amp sq.ft.) in a chromic acid solution (50g. CrO_3 /1000ml) with a Ti 6-4 coupon as the cathode. 49% w/w HF is added to attain the desired current density.
8. Rinse three times in deionized water.
9. Blow dry with prepurified N_2 gas until visibly dry.

Phosphate/Fluoride Acidic Etch (P/F)

1. Gritblast as above.
2. Wipe with MEK.
3. Soak to Sprex AN-9 solution (30g/1000ml) at 80°C for 15 minutes.
4. Rinse three times in deionized water.
5. Immerse in pickle solution (31ml 49%w/w HF, 213ml conc. HNO_3 /1000ml) at room temperature for 2 minutes.
6. Rinse three times in deionized water.
7. Soak in phosphate/fluoride solution (50.5g Na_3PO_4 , 20.5g KF, 29.1ml 49%w/w HF/1000ml) at room temperature for 2 minutes.

8. Rinse three times in deionized water.
9. Soak in deionized water at 65°C for 15 minutes.
10. Blow dry in prepurified N₂ until visibly dry.

TURCO Basic Etch

1. Gritblast as above.
2. Wipe with MEX.
3. Soak in TURCO 5578 solution (37.6g/1000ml) at 70-80°C for 5 minutes.
4. Rinse three times in deionized water.
5. Soak in TURCO 5578 solution (360g/1000ml) at 80-100°C for 10 minutes.
6. Rinse three times in deionized water.
7. Soak in deionized water at 60-70°C for 2 minutes.
8. Blow dry in prepurified N₂ until visibly dry.

Sodium Hydroxide Procedure

1. Rinse with MeOH, acetone, air dry
2. Immerse in Super Terj (30g/l) at 80°C for 15 minutes
3. Soak in water at 50 - 60°C for 15 minutes
4. Anodize in NaOH solution (5.0M)
 - Stainless steel mesh cathod
 - 20 C
 - 10 v
 - Current: for 8 sq. in. immersed, the current was 1c amp initially and decreased to a constant 0.4 amp by 11 minutes.
5. Rinse in running tap water for 20 minutes
6. Dry in oven at 60°C for 10 minutes.

Pretreatment Revisions for Ti-6-4 Foil

CAA

- * One minute in NaOH solution
- * 30 seconds in pickle solution

P/F

- * Five minutes in Super Terj
- * One minute in Pickle
- * One minute in P/F solution

TURCO

- * Two minutes in cleaning solution
- * Five minutes in etchant

Table 1: XPS Data for CAA, P/F, TURCO, SHA and PSHA pretreated surfaces

Pretreatment	XPS	Element	Binding Energy	Atomic Fraction
CAA	KRATOS	C	285.0	51.9
		O	530.0	35.7
		Ti	458.9	10.6
		F	685.3	1.8
CAA	KRATOS	C	285.0	48.0
		O	530.3	37.4
		Ti	458.7	11.4
		F	684.7	3.2
CAA	PHI	C	285.0	48.2
		O	530.2	43.2
		Ti	458.8	6.5
		F	684.8	2.0
P/F	KRATOS	C	285.0	40.4
		O	529.7	46.0
		Ti	458.3	12.2
		P	133.0	1.4
P/F	PHI	C	265.0	38.3
		O	530.4	53.9
		Ti	458.8	6.9
		P	133.5	0.9

Pretreatment	XPS	Element	Binding Energy	Atomic Fraction
TURCO	KRATOS	C	285.0	44.7
		O	529.8	43.5
		Ti	458.1	7.2
		Si	104.1	4.7
		Fe	710.4	trace
TURCO	PHI	C	285.0	44.3
		O	530.4	48.0
		Ti	458.8	4.3
		Fe	711.5	3.5
SHA	KRATOS	C	285.0	31.1
		O	529.9	46.4
		Ti	458.3	8.1
		F	688.5	0.8
			685.5	
		Si	102.8	8.5
		P	133.2	1.4
		Ca	347.1	3.8
SHA	PHI	C	285.0	23.5
		O	530.3	67.4
		Ti	458.7	6.4
		Si	102.9	6.4
		Ca	347.3	1.6

Pretreatment	XPS	Element	Binding Energy	Atomic Fraction
PSHA	KRATOS	C	285.0	36.5
		O	530.5	45.1
		Ti	458.8	10.9
		F	689.1	1.4
		Si	102.3	1.4
		P	133.7	1.9
		Ca	347.4	2.8
PSHA	PHI	C	285.0	28.8
		O	530.3	63.5
		Ti	458.7	6.0
		Ca	347.4	1.7
		Si		trace

TABLE II
SURFACE PRETREATMENT CHEMICAL REPRODUCIBILITY

PRETREATMENT	ELEMENT	<A.F.>	± 95%	<B.E.>	± 95%
CAA	C	49.3	7.2	285.0	--
	O	37.1	4.6	530.4	0.1
	Ti	10.6	2.7	458.8	0.1
	F	2.5	0.8	685.0	0.2
P/F	C	46.8	10.4	285.0	--
	O	41.1	9.0	500.2	0.3
	Ti	9.5	2.6	458.6	0.2
	P	1.9	0.7	133.1	0.3
TURCO	C	52.1	9.0	285.0	--
	O	35.9	8.3	530.0	0.5
	Ti	4.9	1.4	458.5	0.3
	Si	6.2	6.4	104.2	0.7
	Fe	1.3	1.6	712.2	2.7

TABLE III: AES Wide Scan Elements and Kinetic Energies
(K.E.) for CAA, P/F, TURCO, SHA, and PSHA
Pretreated Surfaces

Pretreatment	Element	(K.E.)
CAA	C	266
	O	512,486
	Ti	414,382
	F	658,632
P/F	C	272
	O	512,494
	Ti	412,382
	F	112
TURCO	C	272
	O	512,494
	Ti	418,382
	Fe	702,648
	Si	94
SHA	C	272
	O	512,494
	Ti	418,386
	Ca	294
	Si	80
	P	120
PSHA	C	272
	O	512,496
	Ti	418,384
	Ca	294
	P	120

TABLE IV: SIMS results for CAA pretreated surfaces

Mass/Charge	+ SIMS CAA Possible Assignment
16.0	C^+
19.0	F^+
23.0	Na^+
24.0	C_2^+, Ti^{++}
27.0	Al^+
28.0	N_2^+
39.0	NaO^+
.0	AlO^+
46.0	Ti^+
47.0	Ti^+, TiH^+
48.0	Ti^+, TiH^+
49.0	Ti^+, TiH^+
50.0	Ti^+, TiH^+
51.0	TiH^+, V^+
52.0	Cr^+
56.0	Fe^+
62.0	TiO^+
63.0	$TiO^+, TiOH^+$
64.0	$TiO^+, TiOH^+$
65.0	$TiO^+, TiOH^+$
66.0	$TiO^+, TiOH^+$
67.0	$TiOH^+, VO^+$
68.0	CrO^+
69.0	
80.0	TiO_2^+

TABLE V: SIMS results for P/F pretreated surface

Mass/Charge	+ SIMS P/F Possible Assignment
16.0	O^+
19.0	F^+
23.0	Na^+
24.0	C_2^+, Ti^{++}
27.0	Al^+
28.0	N_2^+
29.0	
32.0	O_2^+
39.0	NaO^+
40.0	Ar^+
41.0	
.0	AlO^+
44.0	SiO^+
46.0	Ti^+
47.0	Ti^+, TiH^+
48.0	Ti^+, TiH^+
49.0	Ti^+, TiH^+
50.0	Ti^+, TiH^+
51.0	V^+, TiH^+
52.0	Cr^+
54.0	
56.0	Fe^+
62.0	TiO^+

+ SIMS

P/F

Mass/Charge

Possible Assignment

63.0	$TiO^+, TiOH^+$
64.0	$TiO^+, TiOH^+$
65.0	$TiO^+, TiOH^+$
66.0	$TiO^+, TiOH^+$
67.0	$TiOH^+, VO^+$
68.0	CrO^+
69.0	
70.0	
75.0	AlO_3^+
78.0	TiO_2^+
79.0	TiO_2^+, TiO_2H^+
80.0	TiO_2^+, TiO_2H^+
81.0	TiO_2^+, TiO_2H^+
82.0	TiO_2^+, TiO_2H^+
83.0	TiO_2H^+, VO_2^+
91.0	
96.0	TiO_3^+

TABLE VI: SIMS results for TURCO pretreated surface

Mass/Charge	+ SIMS TURCO Possible Assignment
16.0	O^+
23.0	Na^+
27.0	Al^+
28.0	N_2^+
40.0	Ar^+
44.0	SiO^+
46.0	Ti^+
47.0	Ti^+, TiH^+
48.0	Ti^+, TiH^+
49.0	Ti^+, TiH^+
50.0	Ti^+, TiH^+
51.0	Ti^+, V^+
52.0	Cr^+
54.0	
56.0	Fe^+
57.0	
62.0	TiO^+
63.0	$TiO^+, TiOH^+$
64.0	$TiO^+, TiOH^+$
65.0	$TiO^+, TiOH^+$
66.0	$TiO^+, TiOH^+$
67.0	$TiOH^+, VO^+$
72.0	FeO^+
80.0	TiO_2^+

TABLE VII: SIMS results for SHA pretreated surface

Mass/Charge	+ SIMS SHA Possible Assignment
7.0	N^{++}
14.0	N^+
16.0	O^+
20.0	HF^+, Ca^{++}
23.0	Na^+
24.0	C_2^+, Ti^{++}
25.0	
26.0	
27.0	Al^+
28.0	N_2^+, Si^+
29.0	
30.0	
32.0	O_{2+}
39.0	NaO^+
40.0	Ca^+, Ar^+
41.0	
42.0	
43.0	AlO^+
44.0	SiO^+
45.0	
46.0	Ti^+
47.0	Ti^+, TiH^+
48.0	Ti^+, TiH^+

+ SIMS
SHA

Mass/Charge

Possible Assignment

49.0	$\text{Ti}^+, \text{TiH}^+$
50.0	$\text{Ti}^+, \text{TiH}^+$
51.0	TiH^+, V^+
56.0	$\text{Fe}^+, \text{CaO}^+$
57.0	
58.0	
59.0	
60.0	SiO_2^+
62.0	TiO^+
63.0	$\text{TiO}^+, \text{TiOH}^+$
64.0	$\text{TiO}^+, \text{TiOH}^+$
65.0	$\text{TiO}^+, \text{TiOH}^+$
66.0	$\text{TiO}^+, \text{TiOH}^+$
67.0	$\text{TiOH}^+, \text{VO}^+$
72.0	CaO_2^+
80.0	TiO_2^+
88.0	CaO_3^+

TABLE VIII: SIMS results for PSHA pretreated surfaces

Mass/Charge	+ SIMS P.SHA Possible Assignment
7.0	N^+
16.0	O^+
20.0	Ca^{++}, HF^+
23.0	Na^+
24.0	C_2^+
25.0	
26.0	
27.0	Al^+
28.0	N_2^+, Si^+
39.0	NaO^+
40.0	Ca^+, Ar^+
41.0	
42.0	
.0	AlO^+
44.0	SiO^+
45.0	
46.0	Ti^+
47.0	Ti^+, TiH^+
48.0	Ti^+, TiH^+
49.0	Ti^+, TiH^+
50.0	Ti^+, TiH^+
51.0	TiH^+, V^+
56.0	Fe^+, CaO^+
57.0	
59.0	
60.0	
62.0	TiO^+
63.0	$TiO^+, TiOH^+$
64.0	$TiO^+, TiOH^+$
65.0	$TiO^+, TiOH^+$
66.0	$TiO^+, TiOH^+$
67.0	$TiOH^+, VO^+$
80.0	TiO_2^+

TABLE IX: SIMS results for TiO_2 powder pressed in indium foil

+ SIMS
 TiO_2 POWDER

Mass/Charge	Possible Assignment
16.0	O^+
23.0	Na^+
26.0	
27.0	
32.0	O_2^+
39.0	NaO^+
40.0	Ar^+
46.0	Ti^+
47.0	$\text{Ti}^+, \text{TiH}^+$
48.0	$\text{Ti}^+, \text{TiH}^+$
49.0	$\text{Ti}^+, \text{TiH}^+$
50.0	$\text{Ti}^+, \text{TiH}^+$
51.0	TiH^+
56.0	Fe^+
62.0	TiO^+
63.0	$\text{TiO}^+, \text{TiOH}^+$
64.0	$\text{TiO}^+, \text{TiOH}^+$
65.0	$\text{TiO}^+, \text{TiOH}^+$
66.0	$\text{TiO}^+, \text{TiOH}^+$
67.0	TiOH^+
78.0	TiO_2^+
80.0	$\text{TiO}_2^+, \text{TiO}_2\text{H}^+$
81.0	$\text{TiO}_2^+, \text{TiO}_2\text{H}^+$
113.0	
115.0	In^+
128.0	

TABLE X. Indicator Dye Test Results

ACID/BASICITY

	Bromphenol Blue	Bromocresol Purple	Bromthymol Blue	Orange 1	Thymol Blue
pH	3.4 - 4.6	5.2 - 6.8	6.0 - 7.6	7.6 - 8.9	8.0 - 9.6
	Y B	Y B	Y B	O V	Y B
CAA ^w	gn. blue	yellow	blue	orange	yellow
CAA ^d	yellow	yellow	orange	orange	orange
P/F	green	yellow	blue	orange	yellow
TURCO	blue	gn. yellow	blue	orange	g.yellow
P.TURCO ^w	dk. blue	yellow	blue	orange	g.yellow
P.TURCO ^d	blue	yellow	blue	orange	yellow
SHA	blue	blue	blue	d.orange	d.green

w: wet
d: dry

TABLE XI: Roughness measurement by profilometry of Ti-6-4 foil
and lap shear coupon surfaces

Ti-6-4 Foil

Pretreatment	Average peak to valley (μm)
CAA	0.33
P/F	0.45
TURCO	0.35

Ti-6-4 Coupons

Pretreatment	Average peak to valley (μm)
CAA	2.13
P/F	2.84
TURCO	3.36

TABLE XII: AES Depth Profile

Average time to reach Ti-0 signal intersection

<u>Pretreatment</u>	<u>Ave. Time</u>
CAA	3.27 min
P/F	0.52 min
TURCO	1.15 min
P. TURCO	0.43 min
SHA	64.0 min
P. SHA	9.50 min

TABLE XIII: Surface energy components of pretreated Ti-6-4 surfaces

Pretreatment	γ_s^D	I_{sw}^P
CAA	4.0	19.7
P/F	40.2	53.6
TURCO	31.2	59.4
P.TURCO	75.5	59.4

TABLE XIV: Results of the alkane displacement calculations

Pretreatment	I_{sw}^P	Test Value	Alkane
CAA	19.7	1.64	Hexane
		0.17	Octane
		-0.83	Decane
		-3.58	Hexadecane
P/F	53.6	-1.47	Hexane
		-0.11	Octane
		0.46	Decane
		1.27	Hexadecane
TURCO	59.4	-0.93	Hexane
		-0.06	Octane
		0.23	Decane
		0.42	Hexadecane
P.TURCO	59.4	-3.15	Hexane
		-0.26	Octane
		1.15	Decane
		3.89	Hexadecane

TABLE XV: XPS results of CAA pretreated foil before
and after heating to 350°C

Treatment	Element	B.E.	Atomic Fraction	O/Ti
CAA before heating	Carbon	285.0	38.1	3.1
	Oxygen	530.4	42.5	
	Titanium	458.8	13.6	
	Fluorine	684.9	2.8	
	Aluminum	74.0	3.1	
CAA after heating to 350°C	Carbon	285.0	17.5	2.8
	Oxygen	530.8	52.3	
	Titanium	459.4	19.0	
	Fluorine	685.4	6.0	
	Aluminum	74.6	5.2	
CAA after heating to 350°C	Carbon	285.0	35.4	2.6
	Oxygen	530.9	41.6	
	Titanium	459.4	16.1	
	Fluorine	685.5	4.0	
	Aluminum	119.6	3.0	

TABLE XVI: XPS Results of P/F pretreated foil before
and after heating to 350°C

Treatment	Element	B.E.	Atomic Fraction	O/Ti
P/F before heating	Carbon	285.0	28.0	3.7
	Oxygen	530.5	53.1	
	Titanium	458.9	14.2	
	Phosphorous	133.3	3.5	
	Nitrogen	400.5	1.2	
P/F after heating to 350°C	Carbon	285.0	60.5	2.7
	Oxygen	530.7	26.5	
	Titanium	459.0	9.7	
	Phosphorous	133.7	1.4	
	Aluminum	74.3	1.8	
P/F after heating to 350°C	Carbon	285.0	22.6	2.4
	Oxygen	530.8	51.8	
	Titanium	459.3	21.9	
	Phosphorous	133.9	1.6	
	Fluorine	685.1	1.2	
	Aluminum	119.3	0.8	

TABLE XVII: XPS results of TURCO pretreated foil
before and after heating to 350°C

Treatment	Element	B.E.	Atomic Fraction	O/Ti
TURCO before heating	Carbon	285.0	50.3	3.1
	Oxygen	530.3	32.9	
	Titanium	458.6	4.8	
	Nitrogen	397.2	9.5	
	Iron	711.1	1.2	
	Sulfur	169.0	1.2	
TURCO after heating to 350°C	Carbon	285.0	82.6	4.7
	Oxygen	531.4	11.2	
	Titanium	459.1	2.4	
	Nitrogen	396.8	1.9	
	Aluminum	74.1	1.9	
TURCO after heating to 350°C	Carbon	285.0	35.6	2.6
	Oxygen	530.6	43.9	
	Titanium	459.0	16.8	
	Iron	709.9	1.5	
	Aluminum	118.9	2.0	

TABLE XVIII: XPS results of PSHA pretreated foil
before and after heating to 350°C

Treatment	Element	B.E.	Atomic Fraction	O/Ti
PSHA before heating	Carbon	285.0	26.8	7.1
	Oxygen	530.7	57.7	
	Titanium	459.0	8.1	
	Calcium	347.8	7.0	
	Phosphorous	133.9	1.4	
	Silicon	102.4	1.7	
	Magnesium	89.4	1.1	
PSHA after heating to 350°C	Aluminum	74.4	3.6	3.6
	Carbon	285.0	21.6	
	Oxygen	530.8	53.5	
	Titanium	459.3	15.0	
	Calcium	347.9	6.6	
	Fluorine	685.3	0.1	
PSHA after heating to 350°C	Silicon	102.3	2.0	3.1
	Carbon	285.0	22.7	
	Oxygen	530.8	52.0	
	Titanium	459.3	16.6	
	Calcium	347.7	5.9	
	Fluorine	685.1	1.0	
	Silicon	102.3	1.7	

TABLE IXA: Peak Assignments for FTIR spectra
of LICA 38, neat

2960.9	C-H asym. str., -CH ₃
2933.9	C-H asym. str., -CH ₂ -alkanes
2874.1	C-H sym. str., -CH ₃
2862.6	
1466.0	-CH ₂ - scissoring, alkanes CH ₃ asym. bending def.
1381.1	C-H sym. bending def., CH ₃
1145.8	C-O str., alkyl P=O str., bonded alkylphosphates, (RO) ₃ P=O
1033.9	P-O-C str., alkyl phosphates

TABLE IXXb: Peak Assignments for FTIR spectra
of LICA 38, Thin Film

2966.7	C-H asym. str., -CH ₃
2937.8	C-H asym. str., -CH ₂ -alkanes
2876.1	C-H sym. str., -CH ₃
2862.2	
1467.9	-CH ₂ - scissoring, alkanes -CH ₃ asym. bending def.
1383.1	C-H sym. bending def., CH ₃
1114.9	C-O str., alkyl
1060.9	C-O str.

TABLE XX: XPS results of polished Ti 6-4 surface

<u>Element</u>	<u>B.E.</u>	<u>Atomic Fraction</u>
Carbon	285.0	31.3
Oxygen	530.3	60.8
Titanium	458.7	5.9
Silicon	102.0	2.0
Calcium	trace	

TABLE XXI: XPS results of LICA-38 film on
polished Ti-6-4

<u>Element</u>	<u>B.E.</u>	<u>Atomic Fraction</u>
Carbon	285.0	55.1
Oxygen	532.3	40.5
Titanium	459.4	1.5
Phosphorous	133.7	2.8

TABLE XXII: Lap shear reproducibility

	CAA	P/F	TURCO	P.T.
	1950	4800	4250	3100
	2300	4600	4250	1000
	3000	3300	4400	4300
	4500	3400	3950	1000
	5000	1900	6000	2900
	3500	3000	3000	2500
	3680	4600	3000	2750
	3380	3300		3100
	4780			4650
	3900			
	5100			
	4700			
MEAN	3800	3600	4100	2900
STDEV	1050	1000	1000	1100

$$(1) \quad \gamma_{sw} = \gamma_{sh} + \gamma_{hw} \cos\theta_{sh/w} \quad \text{Young's Eqn.}$$

$$(2) \quad \gamma_{sh} = \gamma_s + \gamma_h - 2(\gamma_s^d \gamma_h)^{1/2} \quad \text{Fowkes}$$

$$\gamma_{sw} = \gamma_s + \gamma_w - 2(\gamma_s^d \gamma_w^d)^{1/2} - I_{sw}^p$$

Rearrangement of equations

$$\gamma_w - \gamma_h + \gamma_{hw} \cos\theta_{sw/h} = \underbrace{2(\gamma_s^d)^{1/2} [(\gamma_w^d)^{1/2} - (\gamma_h)^{1/2}]} + I_{sw}^p$$

A plot of the left hand side vs. the underlined portion of the right hand side yields a slope = $2(\gamma_s^d)^{1/2}$ with an intercept = I_{sw}^p .

$$\gamma_s^d = \frac{(\text{slope})^2}{4}$$

- where
- γ_{sw} substrate/water interfacial free energy
 - γ_{sh} substrate/hydrocarbon interface free energy
 - $\theta_{sh/w}$ contact angle of water drop on substrate immersed in hydrocarbon
 - γ_s surface energy of substrate
 - γ_h surface energy of hydrocarbon
 - γ_s^d dispersive component of substrate surface energy
 - γ_w^d dispersive component of water surface energy
 - I_{sw}^p polar contribution of substrate

Figure 1: Calculation of surface energy.

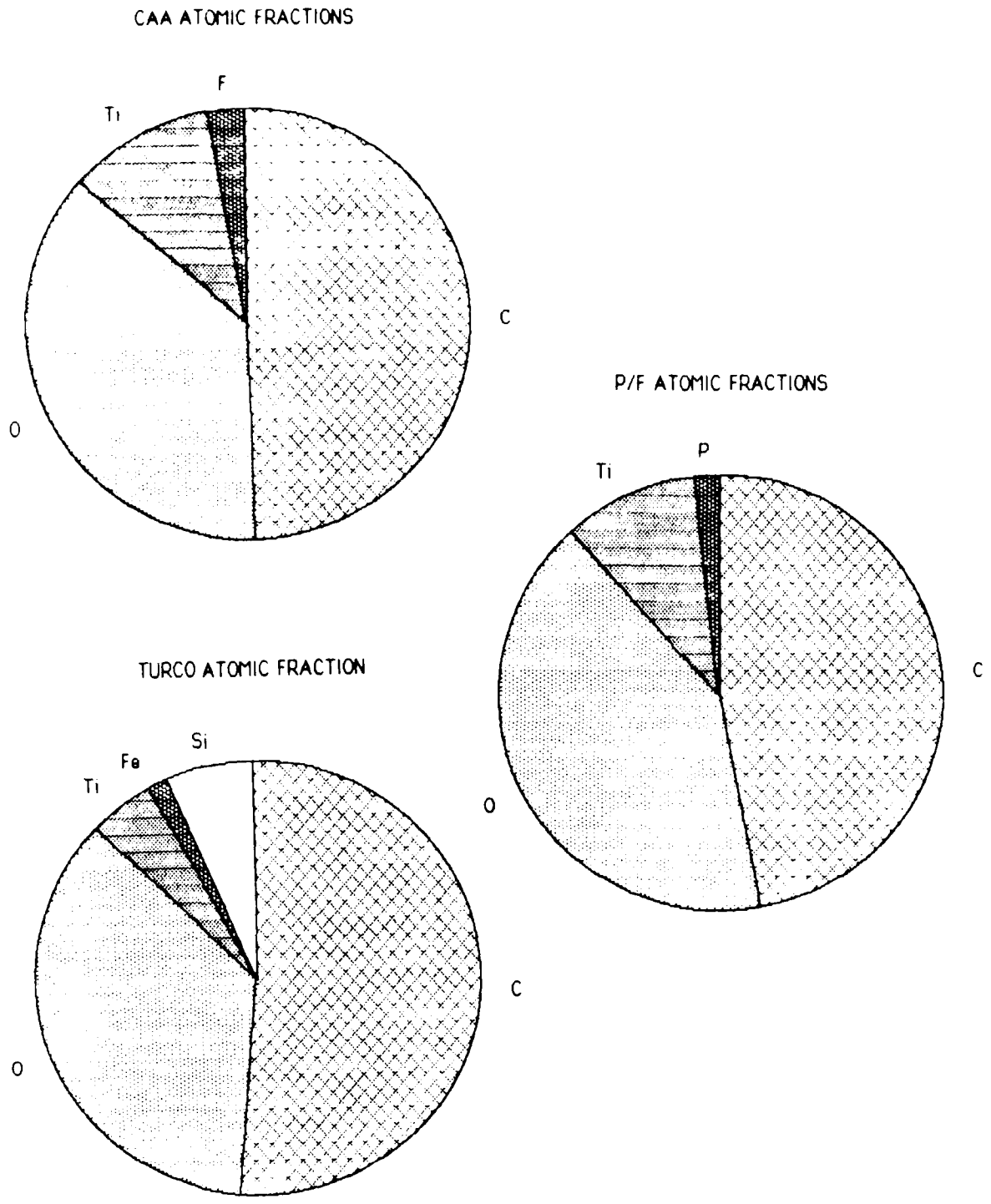


Figure 2: Average atomic fractions of elements present on the surface after each pretreatment.

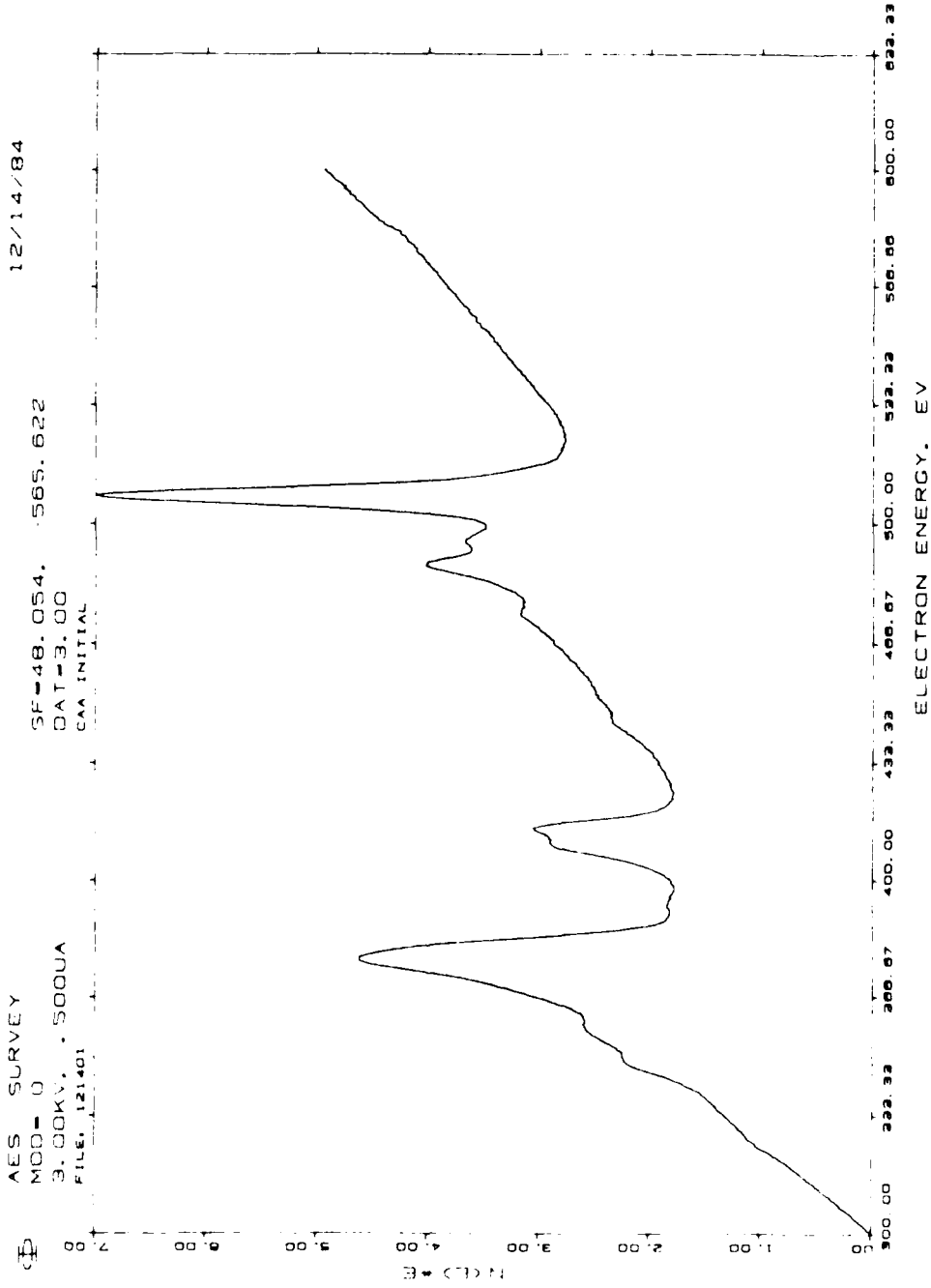


Figure 3: Narrow scan AES of CAA pretreated surface.

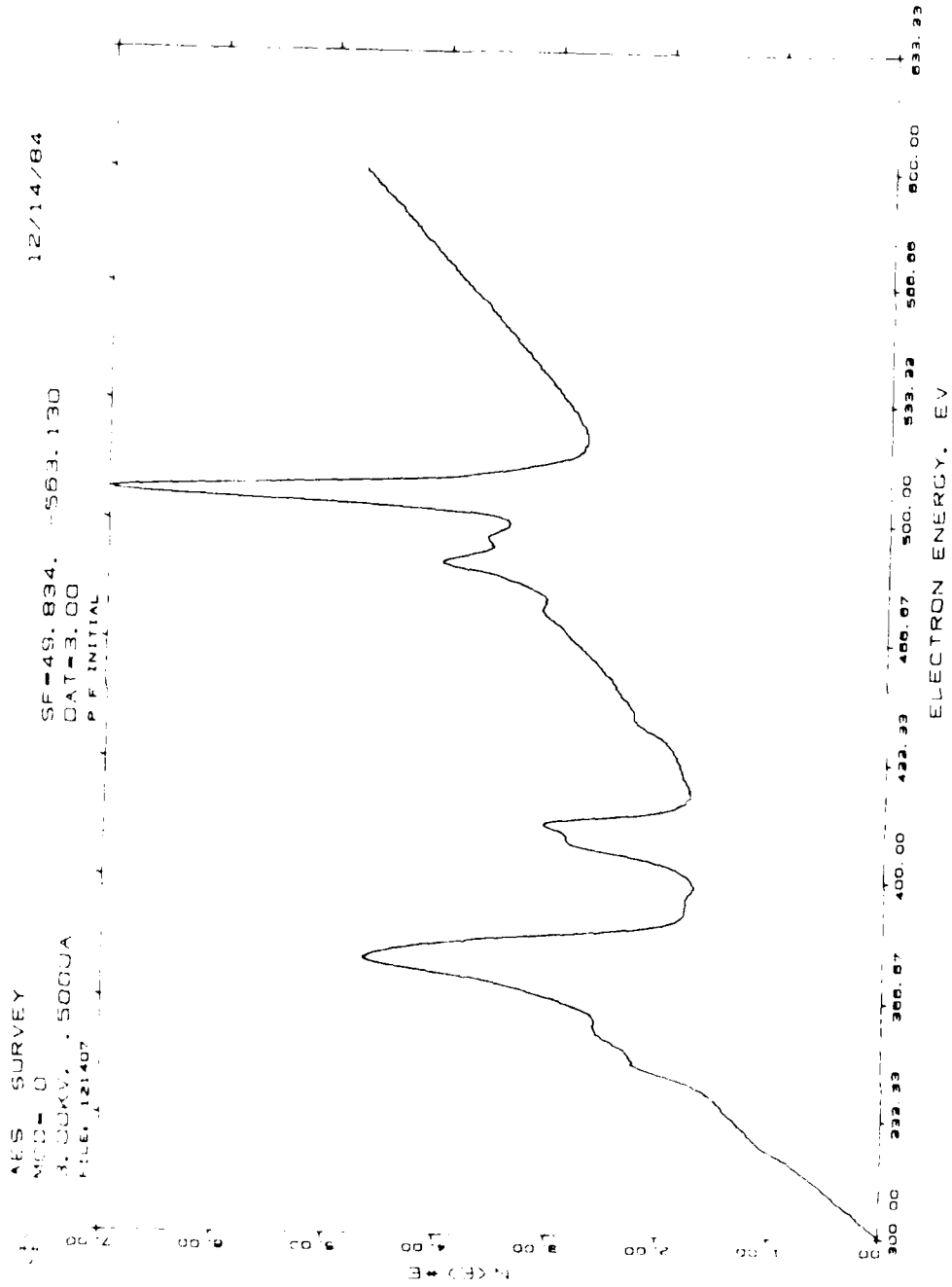


Figure 4: Narrow scan AES of P/F pretreated surface.

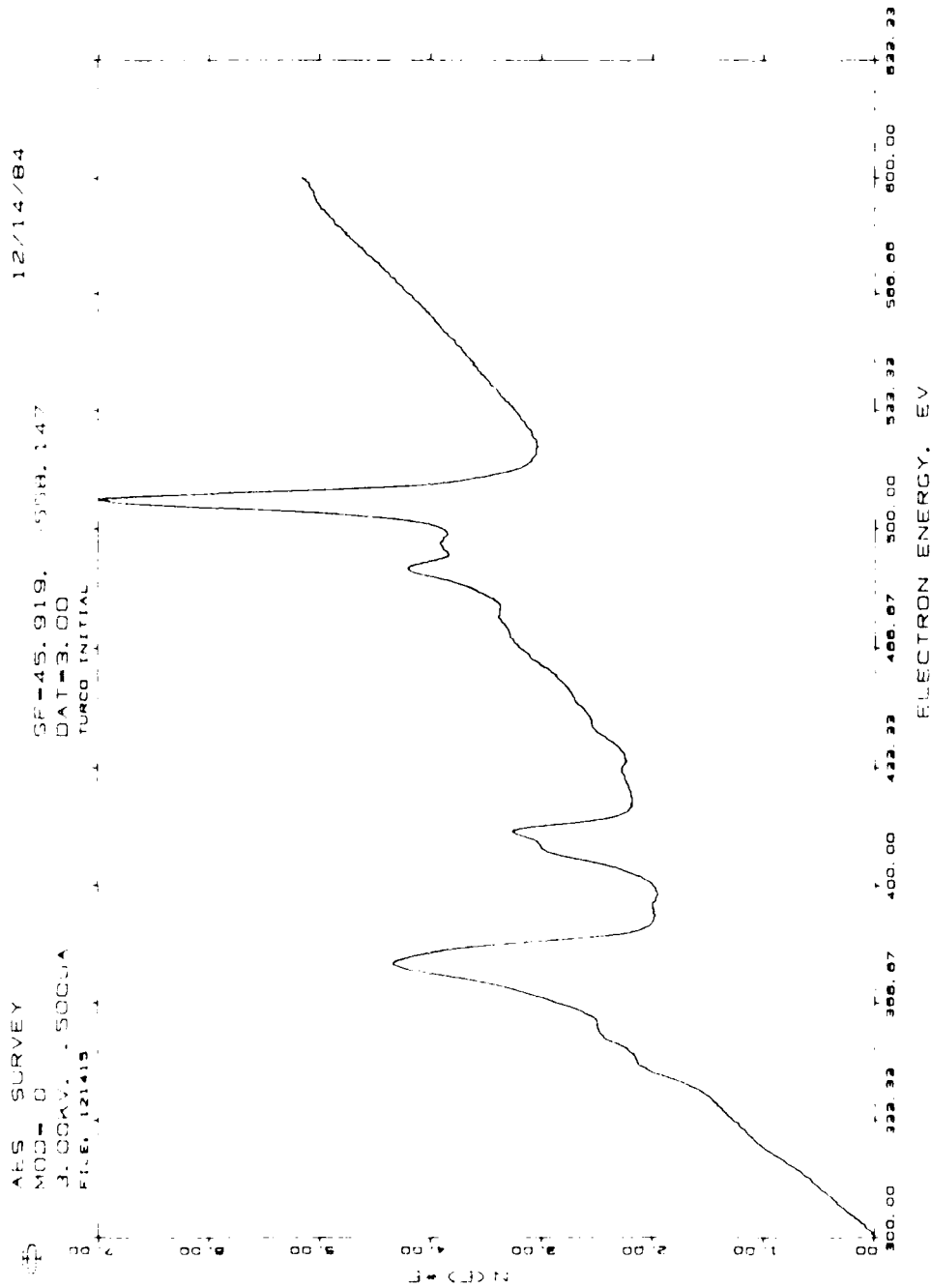


Figure 5: Narrow scan AES of TURCO pretreated surface.

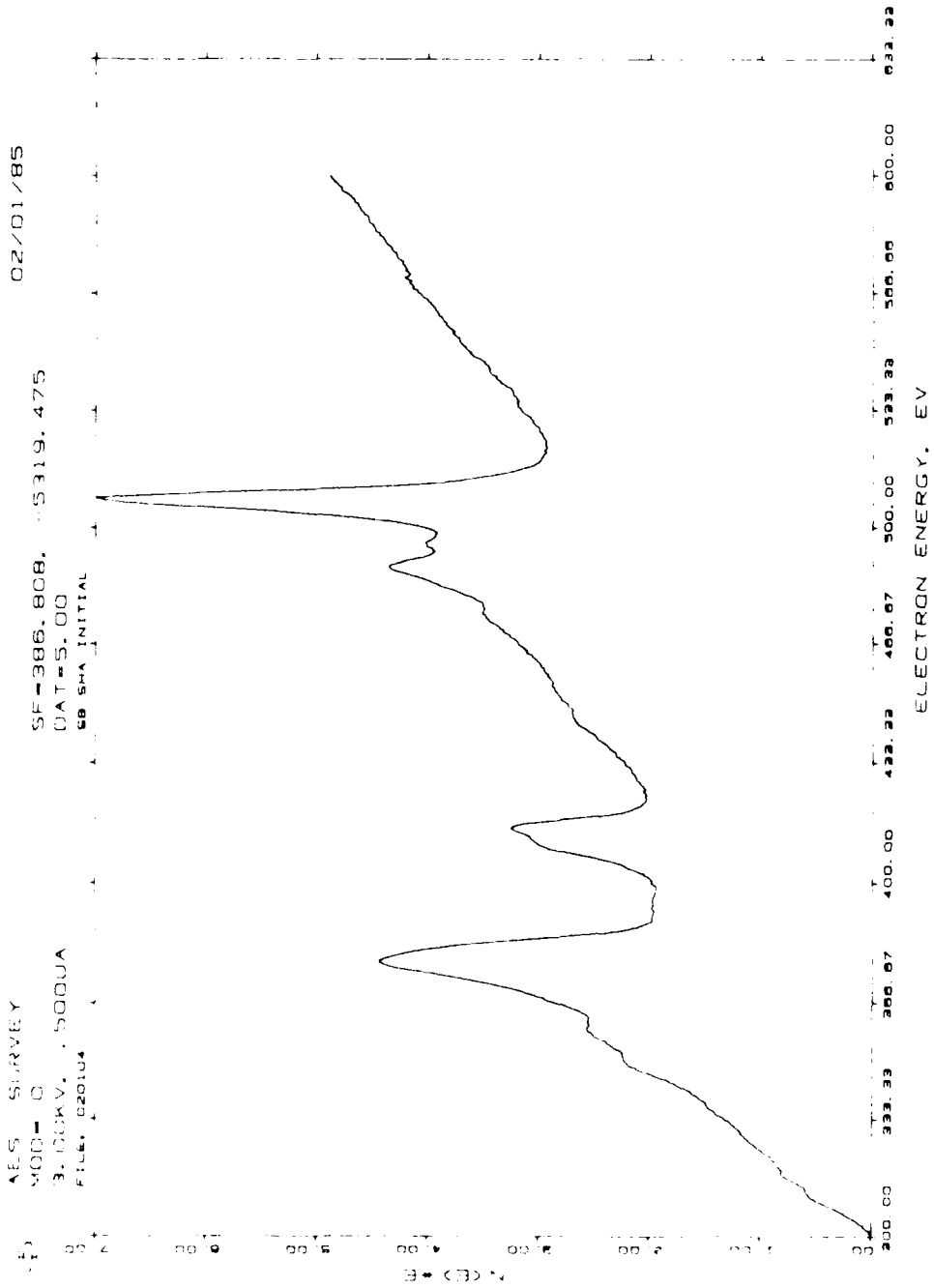


Figure 6: Narrow Scan AES of SHA Pretreated surface.

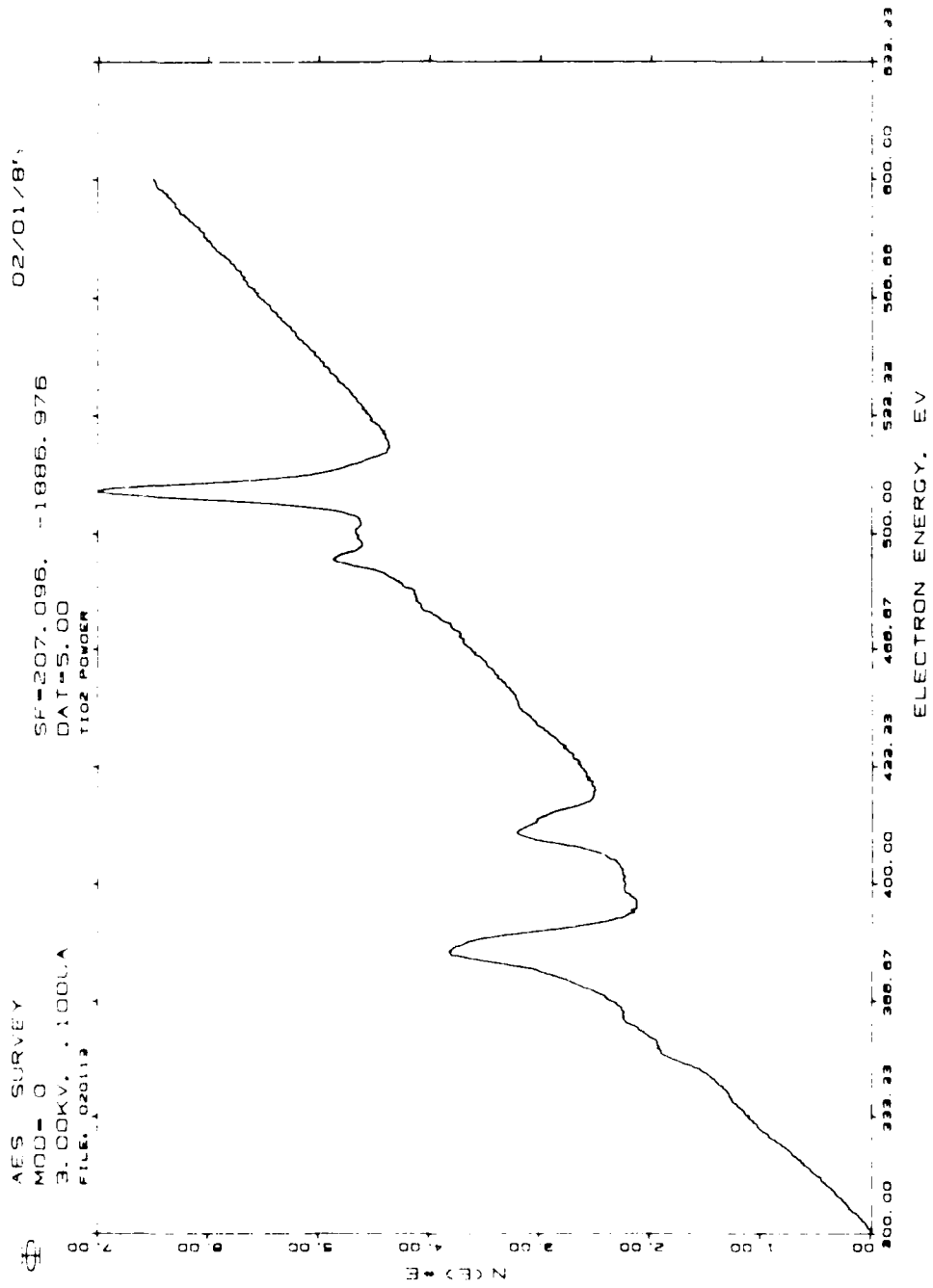


Figure 7: Narrow scan AES of rutile TiO₂ powder.



Figure 8: SEM Stereophotomicrograph taken at 7800 X of SHA pretreated surface.

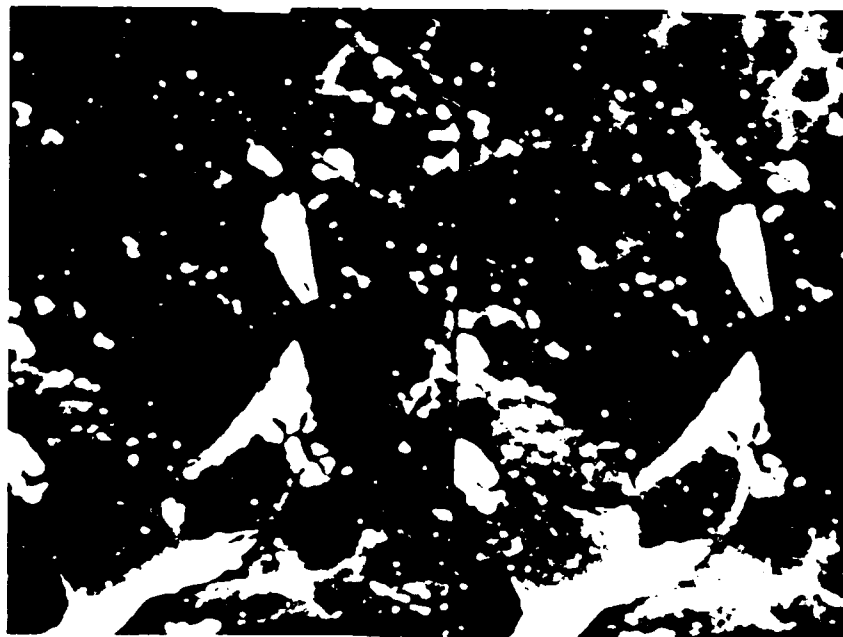


Figure 9: SEM stereophotomicrograph taken at 7800 X of PSHA pretreated surface.

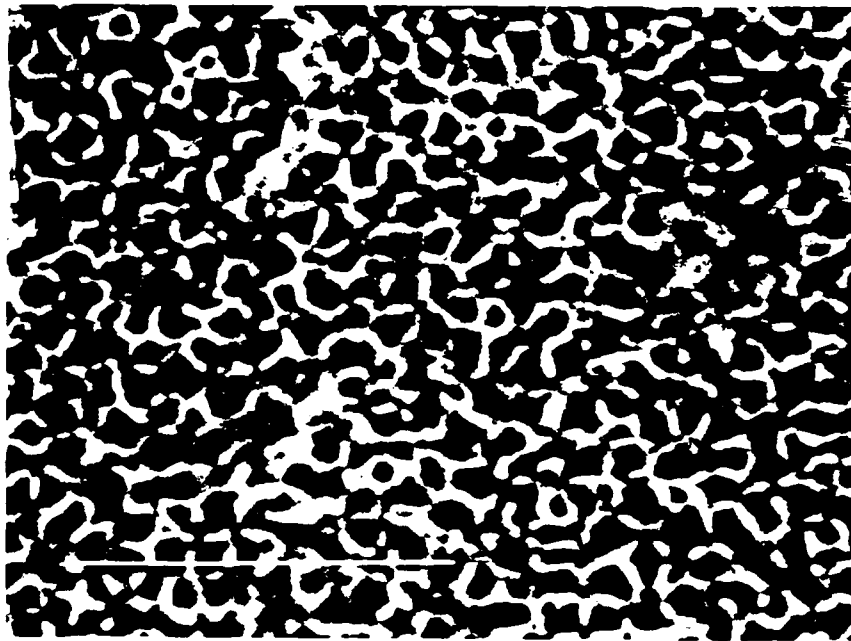


Figure 10: STEM photomicrograph taken at 100,000 of CAA pretreated surface.



Figure 11: STEM photomicrograph taken at 100,000 X of PSHA pretreated surface.

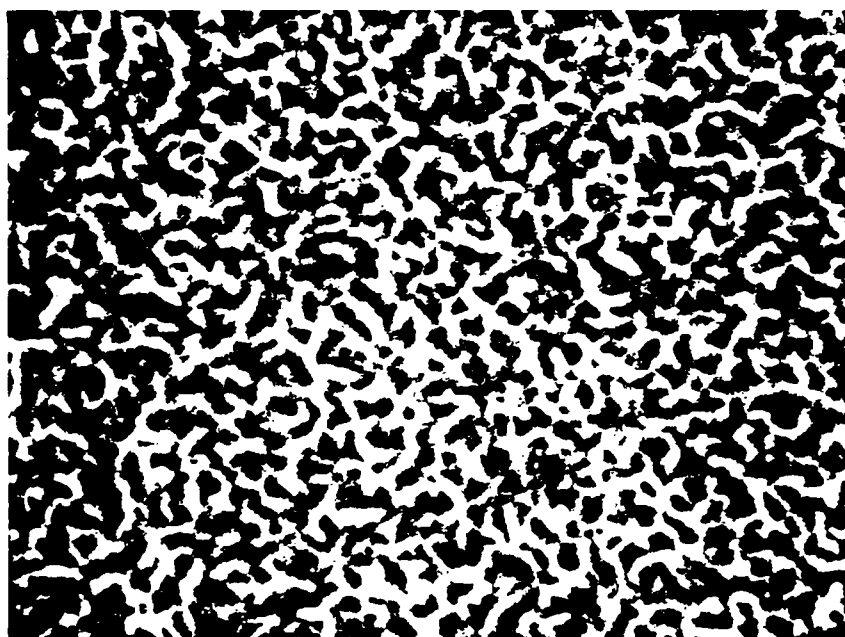


Figure 12: STEM photomicrograph taken at 100,000 X of SHA pretreated surface.



Figure 13: STEM photomicrograph taken at 50,000 X of P/F pretreated surface.

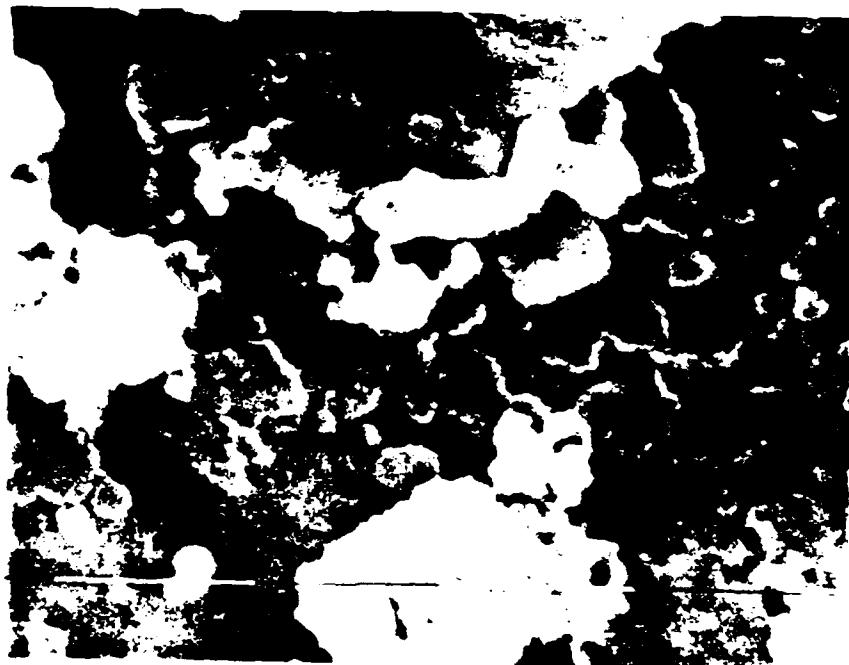


Figure 14: STEM photomicrograph taken at 50,000 X of TURCO pretreated surface.

Surface Energy Determination of CAA

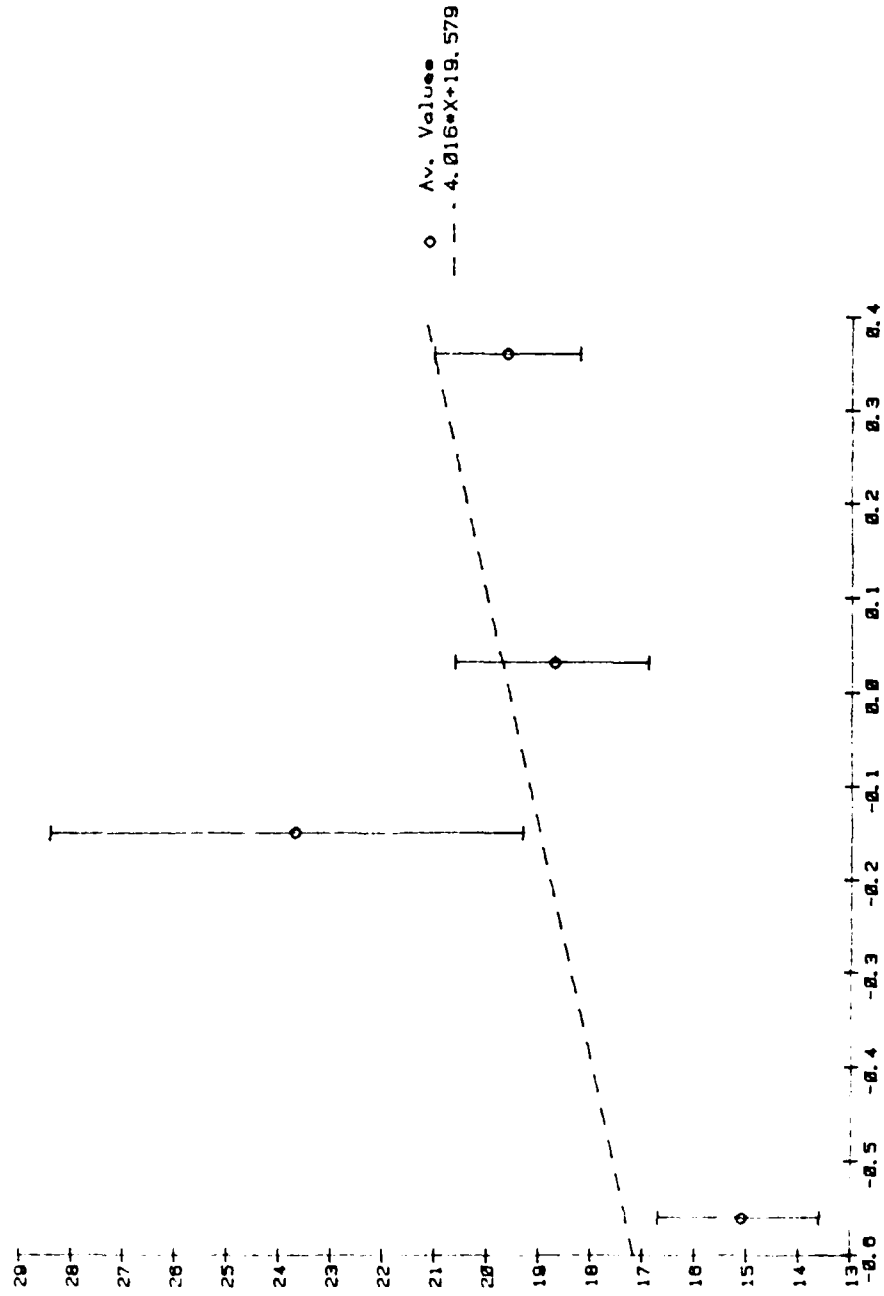


Figure 15: Surface Energy Determination of CAA

$$\gamma_w - \gamma_h + \gamma_{hw} \cos \theta_{sw/h} \text{ vs. } [(\gamma_w^d)^{1/2} - (\gamma_h)^{1/2}]$$

Surface Energy Determination of P/F

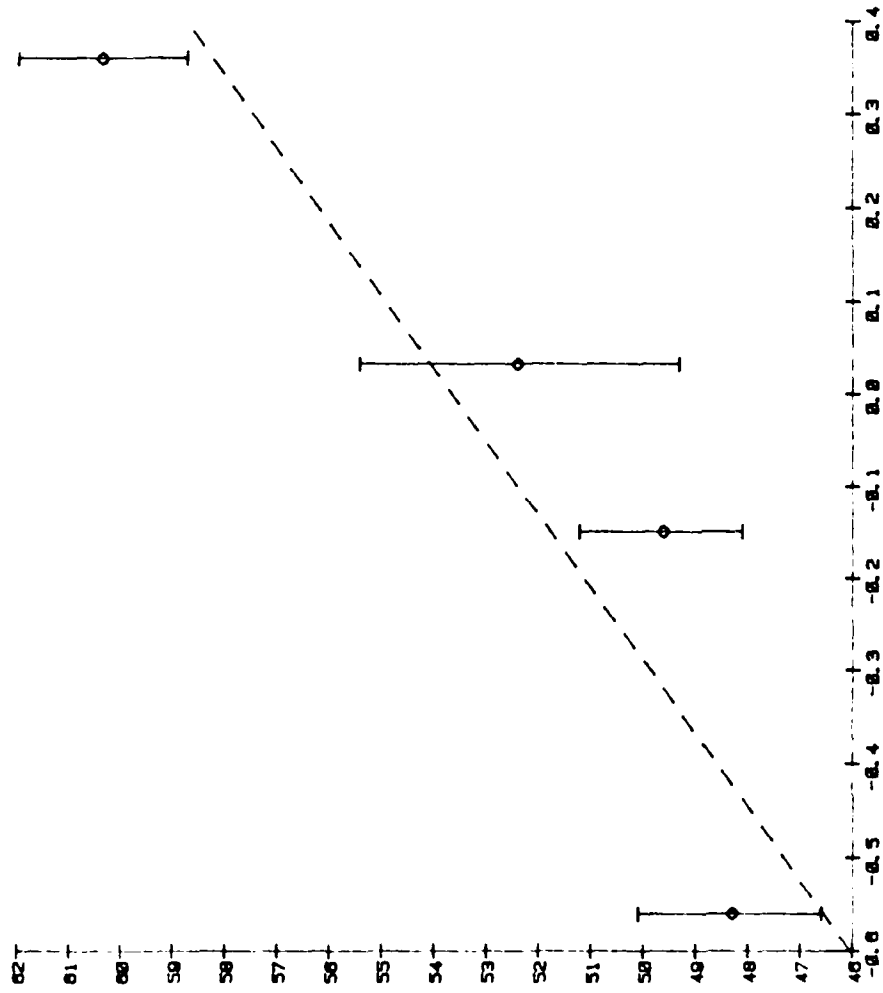


Figure 16: Surface Energy Determination of P/F

$$\gamma_w - \gamma_h + \gamma_{hw} \cos \theta_{sw/h} \text{ vs. } [(\gamma_w^d)^{1/2} - (\gamma_h)^{1/2}]$$

Surface Energy Determination of TURCO

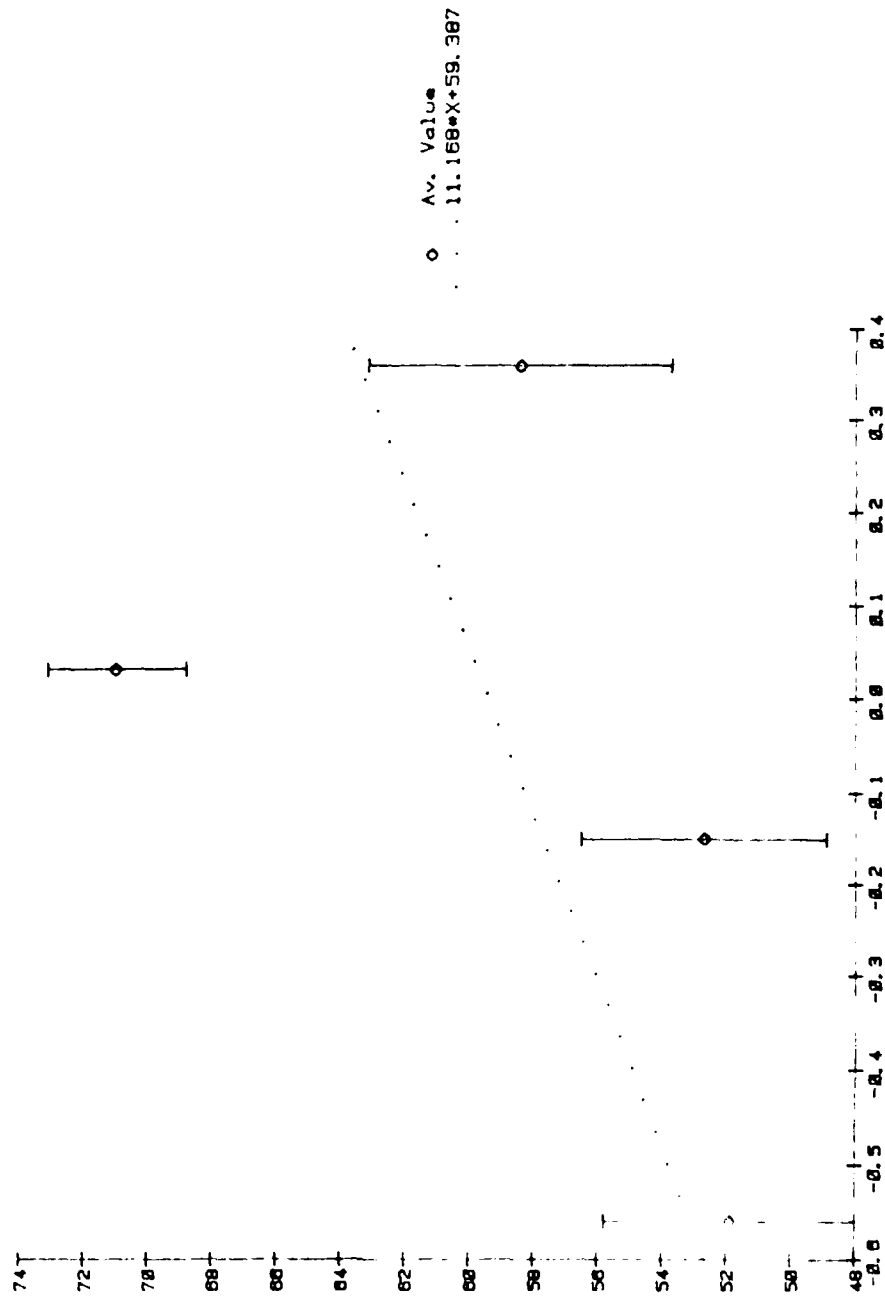


Figure 17: Surface Energy Determination of TURCO

$$\gamma_w - \gamma_h + \gamma_{hw} \cos \theta_{sw/h} \text{ vs. } [(\gamma_w^d)^{1/2} - (\gamma_h)^{1/2}]$$

Surface Energy Determination of P.TURCO

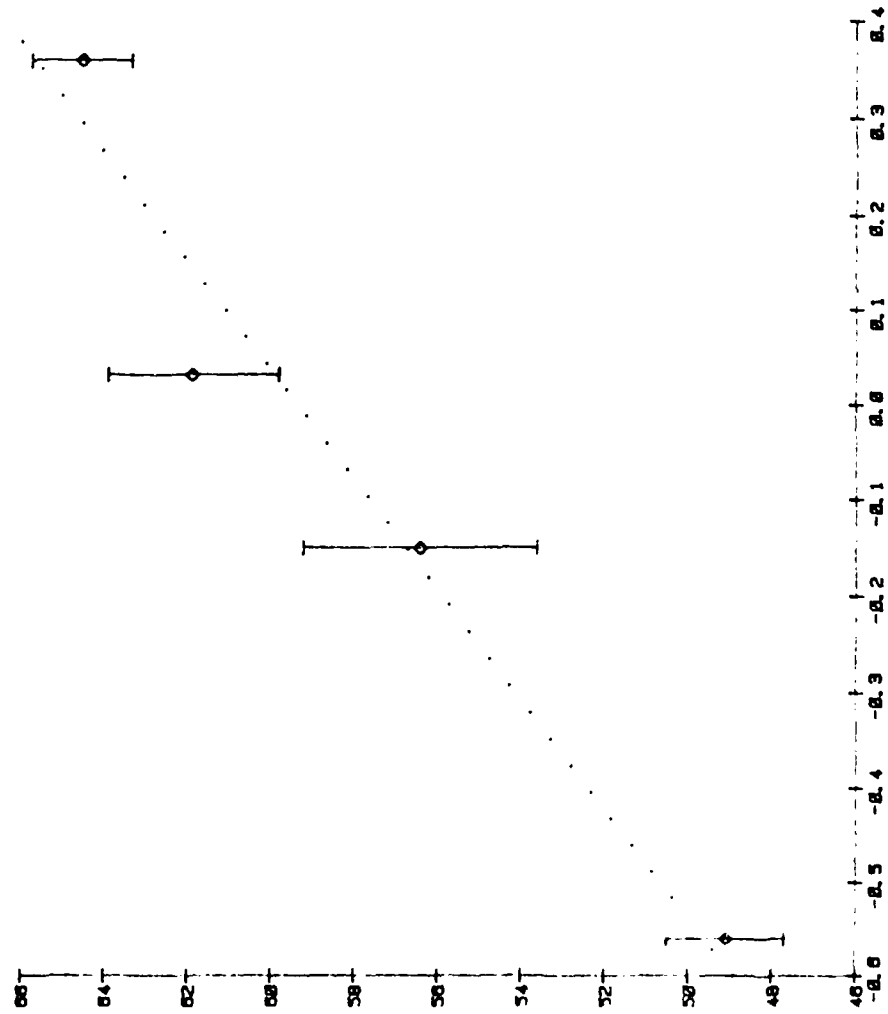


Figure 18: Surface Energy Determination of P.TURCO

$$\gamma_w - \gamma_h + \gamma_{hw} \cos \theta_{sw/h} \text{ vs. } [(\gamma_w^d)^{1/2} - (\gamma_h)^{1/2}]$$

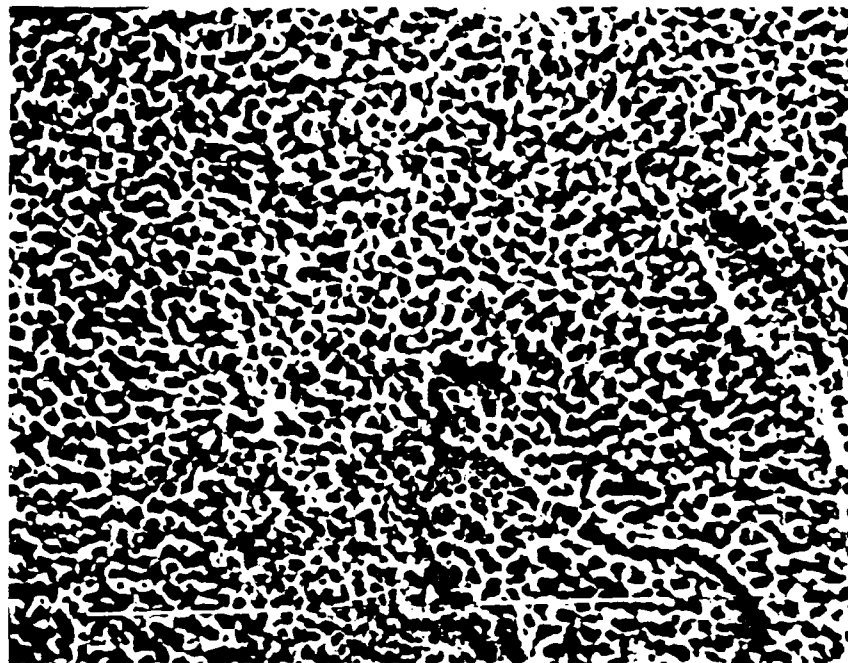


Figure 20: STEM photomicrograph taken at 50,000 X of CAA pretreated surface after heating at 350°C for 10 minutes.

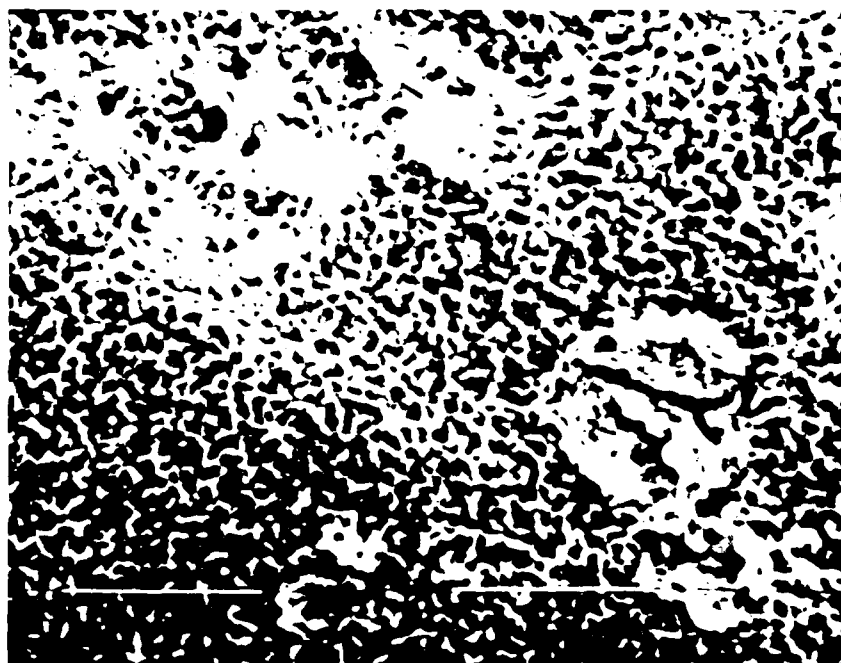


Figure 21: STEM photomicrograph taken at 50,000 X of PSHA pretreated surface after heating at 350°C for 10 minutes.

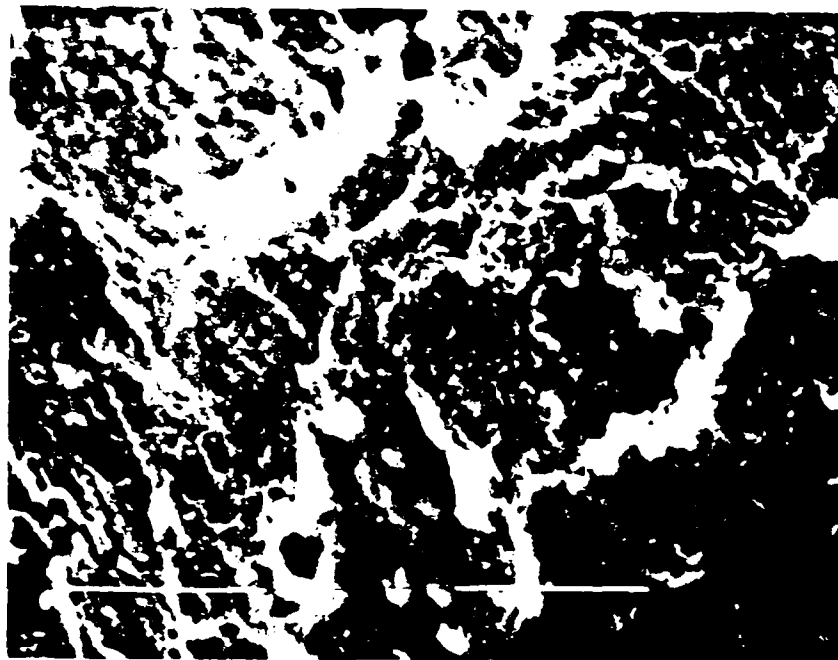


Figure 22: STEM photomicrograph taken at 50,000 X of P/F pretreated surface after heating at 350°C for 10 minutes.

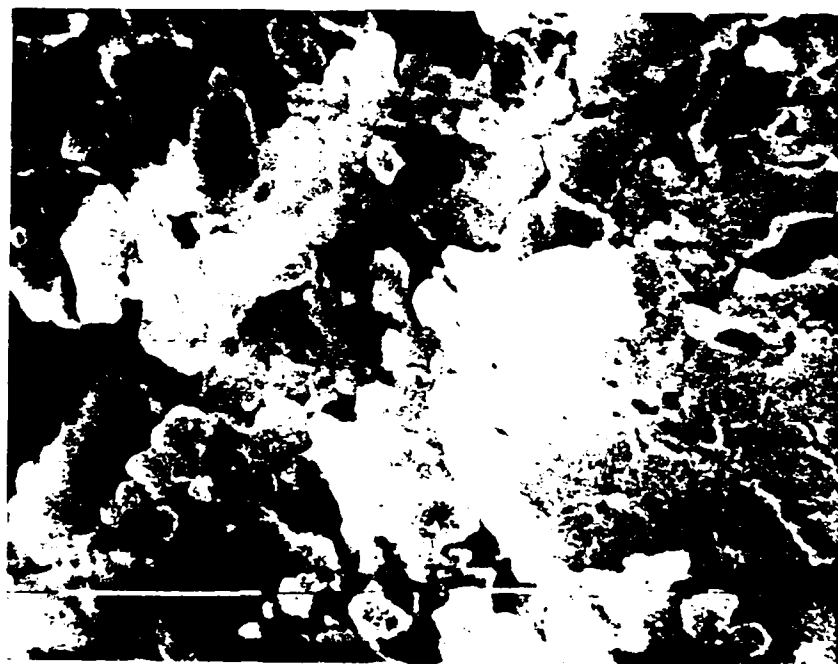


Figure 23: STEM photomicrograph taken at 50,000 X of TURCO pretreated surface after heating at 350°C for 10 minutes.

LICA -38

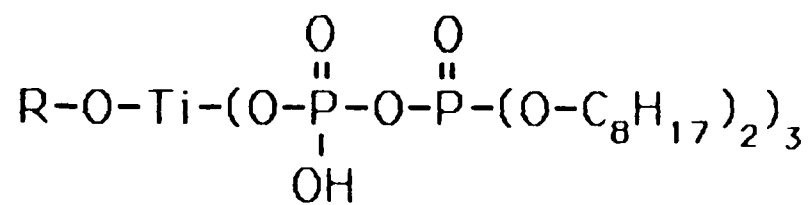


Figure 24: Structure of LICA 38.

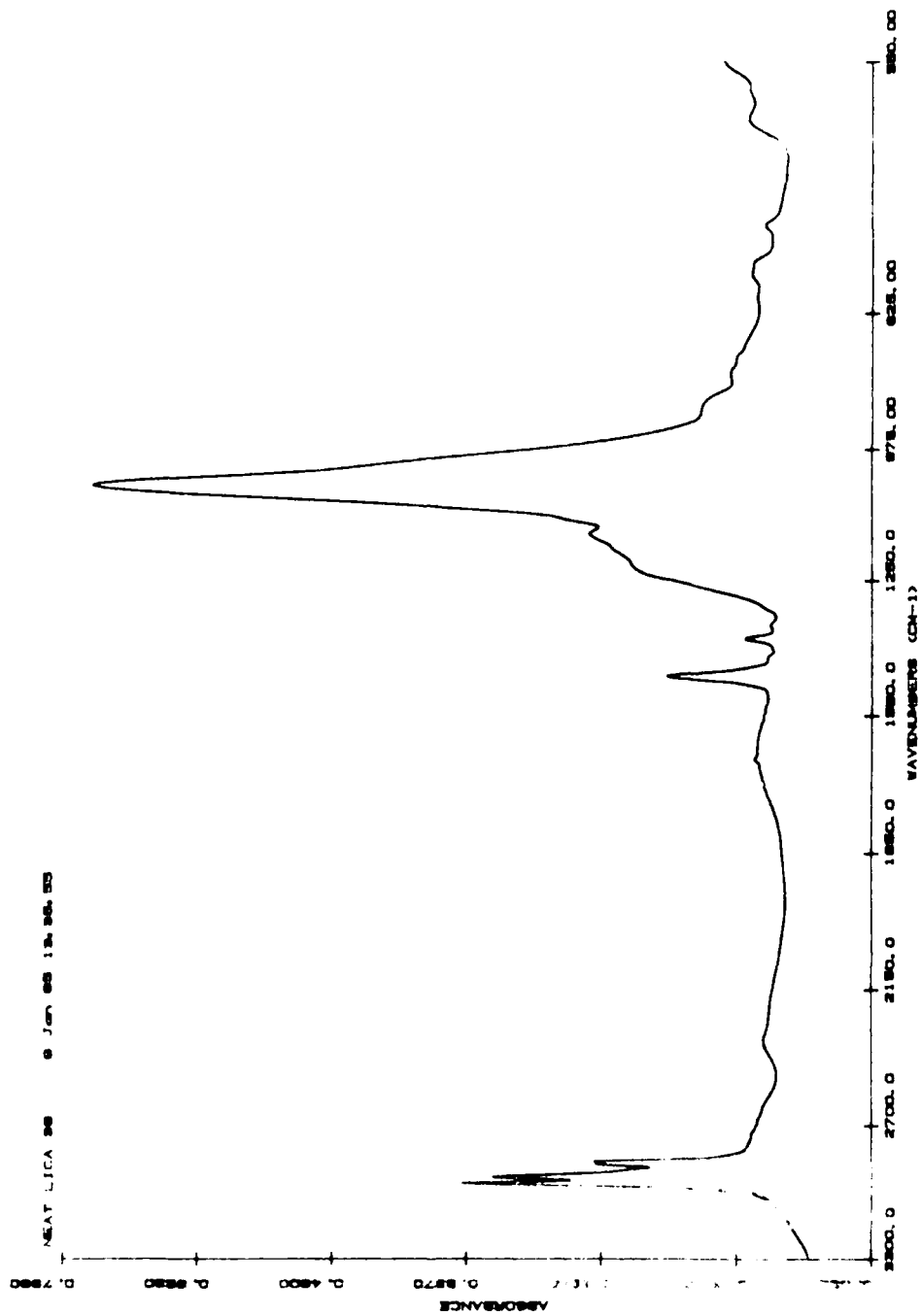


Figure 25: FTIR transmission spectra of LICA 38, neat

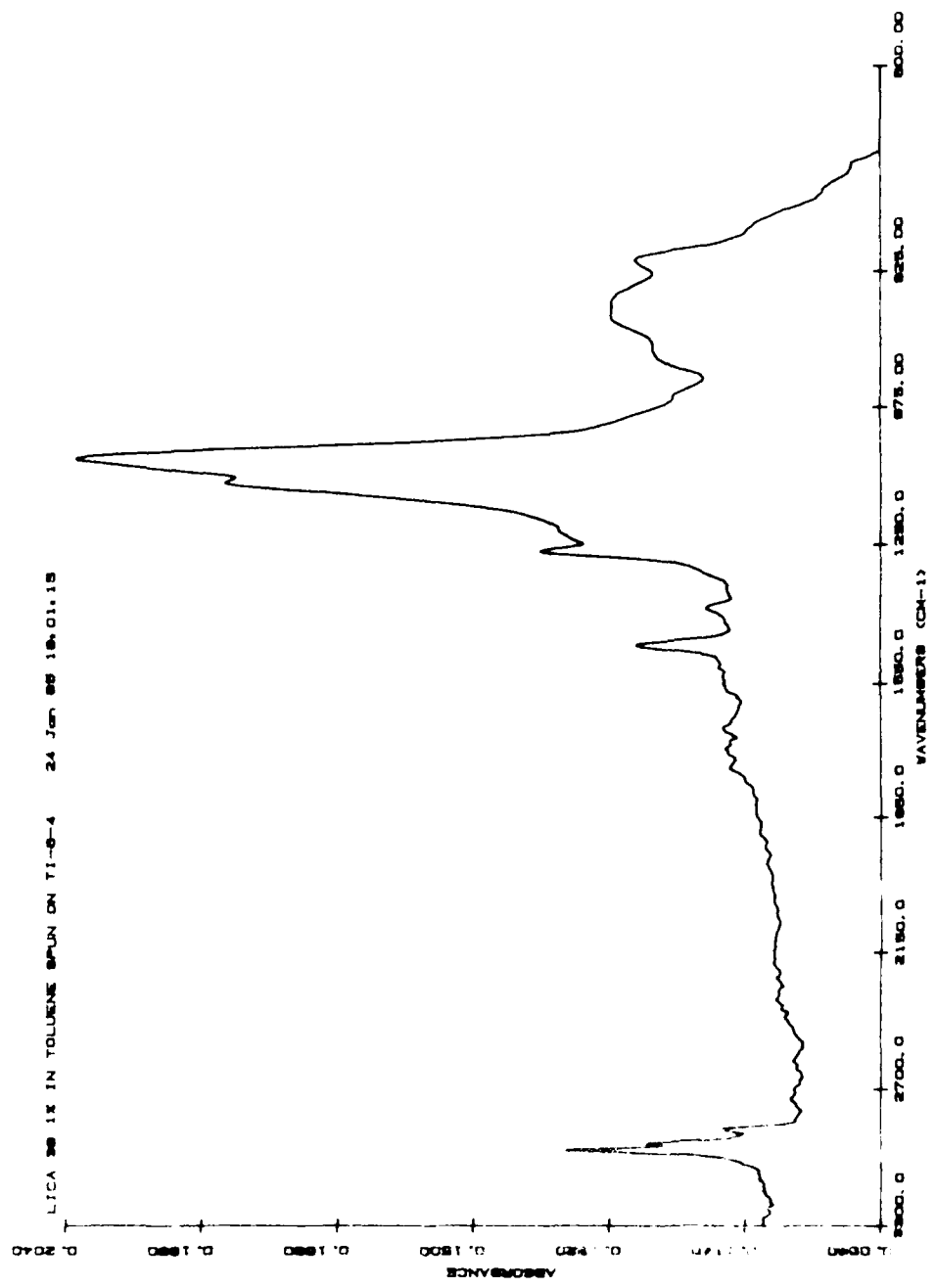


Fig. 26: FTIR grazing angle reflection spectra of LICA 38 film on polished Ti-6-4.

80 C 95% RH

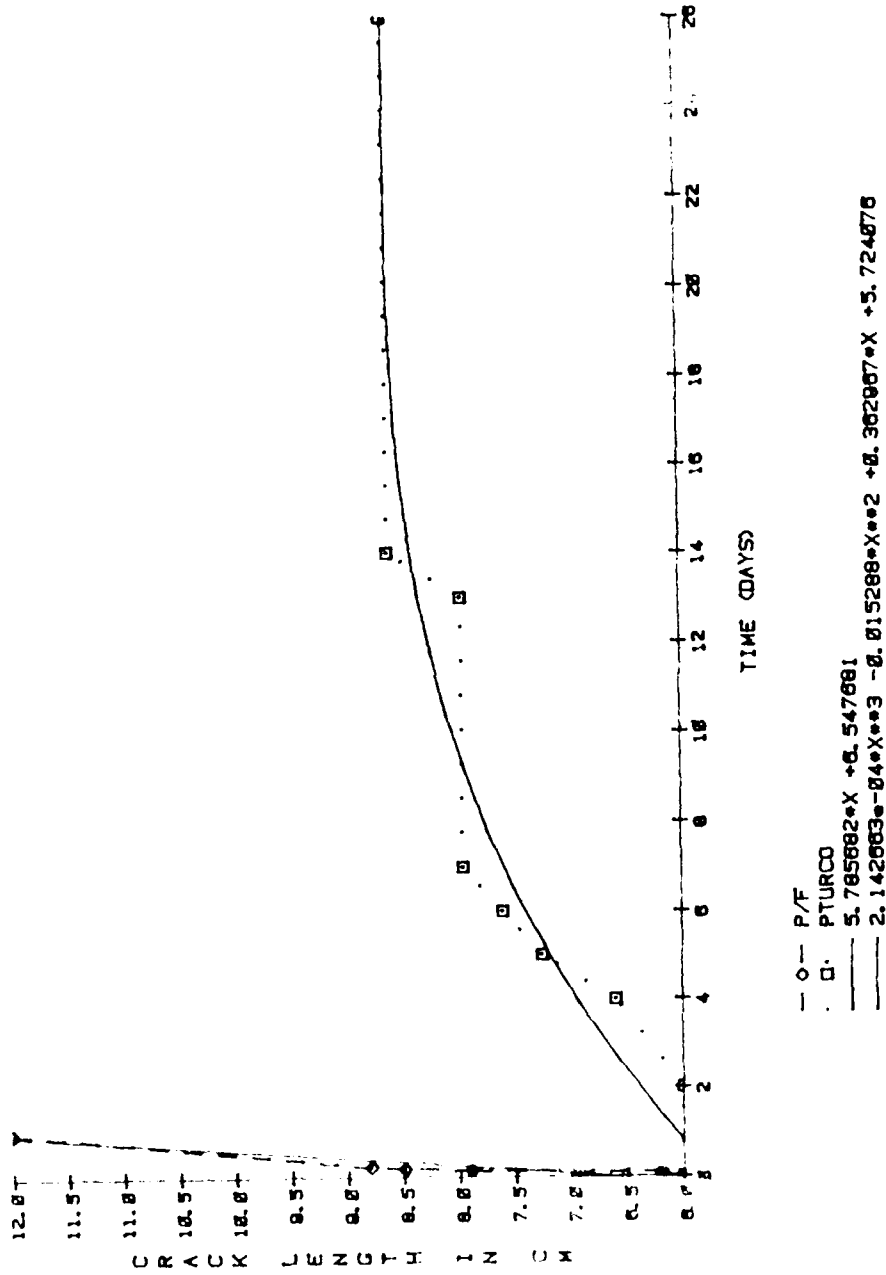


Fig. 27: Crack length vs. time for P/F and P.TURCO pretreated wedge samples in 80°C 95% rh.

80 C 95% RH

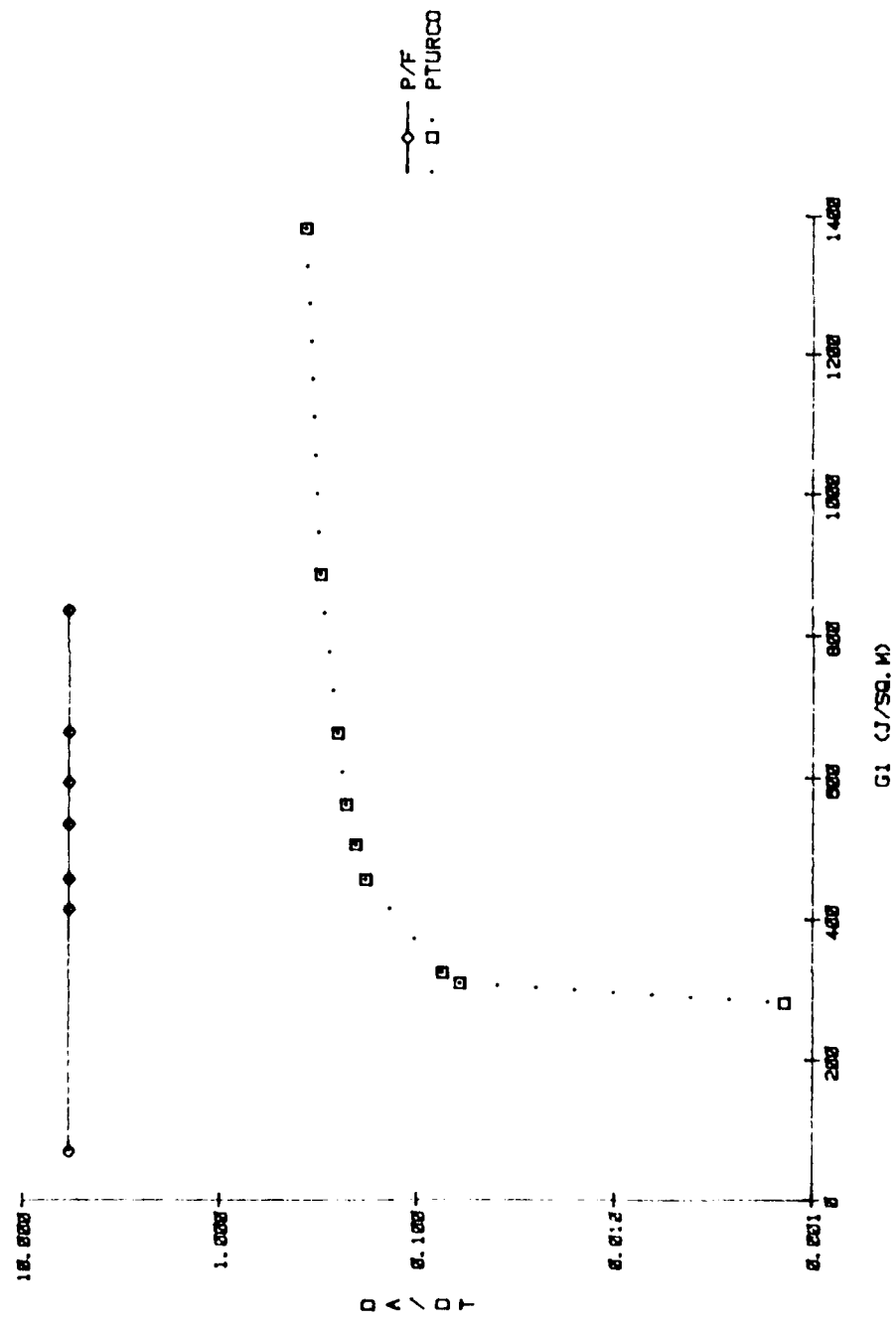


Fig. 28. Rate of crack growth vs. G_I (in J/m^2) for P/F and P.TURCO pretreated wedge samples in 80°C 95% rh.

END

DTIC

8-86